# Soviet Research on the Transport of Intense Relativistic Electron Beams Through High-Pressure Air

Nikita Wells

RAND

The research described in this report was sponsored by the Defense Advanced Research Projects Agency under RAND's National Defense Research Institute, a Federally Funded Research and Development Center supported by the Office of the Secretary of Defense, Contract No. MDA903-85-C-0030.

**Library of Congress Cataloging in Publication Data**

Wells, Nikita, 1937-
Soviet research on the transport of intense relativistic electron beams through high-pressure air.

"Prepared for the Defense Advanced Research Projects Agency."
"May 1987."
Bibliography: p.
"R-3463-DARPA."
1. Electron beams. 2. Plasma (Ionized gases)
3. Electron beams—Research—Soviet Union.
I. United States. Defense Advanced Research Projects Agency. II. RAND Corporation.
III. Title.
QC793.5.E622.W43 1987 537.5'3 86-31496
ISBN 0-8330-0787-4

The RAND Publication Series: The Report is the principal publication documenting and transmitting RAND's major research findings and final research results. The RAND Note reports other outputs of sponsored research for general distribution. Publications of The RAND Corporation do not necessarily reflect the opinions or policies of the sponsors of RAND research.

Published by The RAND Corporation
1700 Main Street, P.O. Box 2138, Santa Monica, CA 90406-2138

R-3463-DARPA

# Soviet Research on the Transport of Intense Relativistic Electron Beams Through High-Pressure Air

Nikita Wells

May 1987

Prepared for the
Defense Advanced Research Projects Agency

RAND

APPROVED FOR PUBLIC RELEASE; DISTRIBUTION UNLIMITED

# PREFACE

This report was prepared in the course of a continuing study of Soviet research and development of high-current, high-energy charged particle beams and their scientific and technological applications. The report examines Soviet research on the propagation of intense relativistic electron beams (IREBs) through high-pressure air and gases ($p > 10^{-2}$ Torr), as reported in Soviet open-source technical publications. A companion RAND report, *Soviet Research on the Transport of Intense Relativistic Electron Beams Through Low-Pressure Air*, R-3309-ARPA, August 1986, by the same author considers Soviet research on the propagation of IREBs through low-pressure air and gases ($10^{-6}$ Torr $< p < 10^{-3}$ Torr).

The report should be of interest to specialists in pulsed-power and high-current charged-particle-beam research.

This study was sponsored by the Defense Advanced Research Projects Agency, Office of the Secretary of Defense (OSD), and was carried out in the Applied Science and Technology Program of the National Defense Research Institute, RAND's OSD-supported Federally Funded Research and Development Center.

# SUMMARY

The Soviets have actively pursued research into the propagation of intense relativistic electron beams (IREB) (beam energies above 450 keV and beam currents in the tens of kA range) through air and other gases since the early 1970s. The present report analyzes the Soviet developments of IREB propagation through background air at pressures from $10^{-2}$ Torr to atmospheric, as reflected by Soviet open source technical literature published over the past 15 years. A previous report by the same author considered Soviet developments on IREB propagation through air at low pressures ($10^{-6}$ to $10^{-3}$ Torr) [1].

Soviet research on IREB propagation in air has greatly increased recently, as evidenced by:

- A large increase in the number of researchers and published papers on IREB propagation from 1980 to 1984.
- A coincident disappearance from publication in any area of science of five important experimental research teams, suggesting censorship action imposed on these teams.

The most important findings of Soviet research seem to match U.S. observations regarding propagation, as follows:

1. The formation of a plasma channel created by an IREB propagating through background air and the effect of beam parameters upon the plasma channel parameters (and vice versa).
2. Determination of the background air pressure for the optimum transport of IREB. Two optimum pressure ranges were determined:
   (a) The "ion focused regime"—0.06 to 0.09 Torr
   (b) The "low pressure window"—1 Torr
3. Observation of current enhancement, whereby the IREB-induced current in plasma is higher than the initial beam current.
4. The effect of resistive hose instability upon IREB propagation.

Both the United States and the USSR are concentrating on the same effects inherent to IREB propagation through air. However, an important difference between the Soviet research, as presented in the open literature, and the U.S. research is that the Soviet high current experiments are carried out with pulsed diode machines in the 1 to 1.5 MeV range and with a poorer quality beam than the U.S. experiments such as on the ATA 50 MeV accelerator and other beams. There is a striking absence of any high energy, high current research in the USSR.

Most Soviet research has been carried out at nine institutes, five of which have made extensive experiments using IREBs with energies of 0.5 to 1.5 MeV, beam currents of 15 to 50 kA, and pulse lengths of 20 to 60 ns, with beam propagation lengths from fractions of a meter to 3 meters. In one case, experiments using beam energies of 2 to 20 MeV were made at low beam currents.

Soviet theoretical investigations on the formation of a plasma channel by the passage of an IREB through air have been carried out by computer simulation made on the BESM-6 computer for cases of a 1 MeV, 30 kA IREB. A new model used was more adapted to higher pressures and longer distances. This model took into account changes in plasma channel parameters due to IREB and changes in beam charge and current density profiles. Pressures considered in this model were from 1 to 100 Torr and the electron energy inside the plasma channel was tens of eV.

According to Soviet researchers, for optimum beam transport through air it is imperative to ensure conditions that allow full neutralization of the IREB's self-fields along the entire path of the beam's transport. The propagation is determined by the plasma channel configuration while the trajectory is determined by movement of electrons that have lower energy than the main component of the electron beam.

Soviet emphasis on IREB propagation through fairly high pressure may be important in light of the recent increased effort. The high pressure range considered in this report is basically applicable to inertial confinement fusion, where the beam must be transported with minimum losses from the accelerator to the target. However, in the case of ICF, the gas through which the beam propagates usually is not air, because propagation through air rather than through other gases (especially He) was found to be much less efficient. This pressure range also applies to the passage of IREB through the atmosphere and is pertinent to endoatmospheric charged-particle beam weapons and other military applications.

# ACKNOWLEDGMENTS

The author would like to thank Martin Lampe of the Naval Research Laboratory and Eugene J. Lauer of the Lawrence Livermore National Laboratory for their reviews of this report and for their many useful suggestions. He is also grateful to his colleagues at The RAND Corporation: Robert W. Salter for reviewing the report; Simon Kassel for direction to, support of, and interest in the project; and Nathan Brooks for assistance in accumulating and organizing the Soviet technical data.

The American Institute of Physics kindly granted permission to reproduce graphics taken from the following Soviet scientific journals: *Soviet Physics—Technical Physics (Zhurnal tekhnicheskoy fiziki)*, graphics appearing herein as Figs. 3–6, 21, 25–27, and 40; *Soviet Journal of Plasma Physics (Fizika plazmy)*, graphics appearing herein as Figs. 7–20, 23–24, and 41–51; *Soviet Physics—JETP (Zhurnal eksperimental'noy i teoreticheskoy fiziki)*, graphics appearing herein as Figs. 28–32; and *Soviet Technical Physics Letters (Pis'ma v Zhurnal tehknicheskoy fiziki)*, graphics appearing herein as Figs. 33–39, and 52.

Plenum Publishing Corporation kindly granted permission to reproduce the graphic taken from the Soviet scientific journal *Soviet Physics Journal (Izvestiya vysshikh uchebnykh zavedeniy: fizika)*, appearing herein as Fig. 22.

# CONTENTS


PREFACE ..... iii

SUMMARY ..... v

ACKNOWLEDGMENTS ..... vii

FIGURES ..... xi

TABLES ..... xv

GLOSSARY ..... xvii

Section

I. INTRODUCTION ..... 1

II. IYAF-TPI RESEARCH ..... 7

Theory and Computer Simulation ..... 7

IYAF-TPI Research—Experiments on Channel Formation and Hose Instabilities ..... 23

III. IAE RESEARCH ON HOSE INSTABILITY ..... 31

IV. FIAN-IOF RESEARCH—EXPERIMENTAL BEAM PROPAGATION STUDIES ..... 37

V. KhFTI EXPERIMENTAL RESEARCH ON BEAM PROPAGATION ..... 45

VI. NIIEFA EXPERIMENTAL RESEARCH—TWO-STREAM INSTABILITY ..... 53

VII. NIITP EXPERIMENTAL RESEARCH—IREB INJECTION INTO ATMOSPHERIC AIR ..... 55

VIII. VEI RESEARCH—THEORY AND EXPERIMENT ..... 56

IX. MFTI RESEARCH ON BEAM INSTABILITY ..... 59

X. IEM RESEARCH ..... 61

XI. CONCLUSIONS ..... 62

Appendix: SOVIET RESEARCH TEAMS INVOLVED IN IREB PROPAGATION ..... 65

REFERENCES ..... 67

# FIGURES


1. Chronology of Soviet Research on IREB Propagation Through Air . . . . . 3
2. Number of Soviet Open Source Papers Published on IREB Propagation Through Air, and the Number of Authors of These Papers as a Function of Years . . . . . 6
3. Axial Profile of the Azimuthal Magnetic Field $B_\theta$ and the Total Current $I_T$ for p = 1 and 10 Torr for times t = 50 ns, 30 ns, and 10 ns . . . . . 8
4. Axial Profile of the Azimuthal Magnetic Field $B_\theta$ in a 1 Meter Long Drift Tube, t = 30 ns . . . . . 8
5. Radial $B_\theta$ Field Distribution for p = 1 Torr, t = 20 ns as a Function of Various Axial Distances . . . . . 9
6. Plasma Density Longitudinal Profile at p = 1 Torr and 10 Torr at Times of: t = 50, 30, and 10 ns . . . . . 9
7. Radial Distribution of the Beam Current Density for Several Background Air Pressures . . . . . 10
8. Total Beam Current Pulse as a Function of Background Pressure and Drift Tube Radius $R_c$ . . . . . 11
9. Time Dependence of the Plasma Density ($n_e$) as a Function of Background Pressure for r = 0 and r = 5 cm . . 11
10. Radial Plasma Density Distribution ($n_e$) as a Function of Background Pressure and Drift Tube Size for a Time of 37 ns After Initiation of the Beam Pulse . . . . . 12
11. Plasma Channel Radius $r_p$ as a Function of Background Pressure for Several Drift Tube Radii . . . . . 13
12. Characteristic Average Plasma Electron Energy ($\epsilon_k$) as a Function of Time and its Radial Distribution at Time t = 37 ns and Drift Tube Radius of 12 cm for Various Background Pressures . . . . . 13
13. The Plasma Electron Density ($n_e$) Distribution Along the Drift Tube with $r_{bo}$ = 1 cm, $R_c$ = 2 cm . . . . . 15
14. Dependence of $n_e$ Upon Time . . . . . 16
15. Dependence of the Characteristic Energy of the Plasma Electrons ($\epsilon_k$) and the Conductivity of the Plasma Channel ($\sigma$) Upon Gas Pressure (p) for r = 0, $r_{bo}$ = 1 cm, $R_c$ = 2 cm . 17
16. Axial Profile of the Azimuthal Magnetic Field $B_\theta$ for r = $r_{bo}$ = 1 cm, $R_c$ = 2 cm . . . . . 18
17. Electron Beam Current Pulse Shape . . . . . 19
18. Dependence of the Beam Radius $r_b$ Upon the Axial Length Z . . . . . 20

19. Relative Beam Current Losses for $r_{bo}$ = 1 cm . . . . . 21
20. Beam Radius $r_b$ as a Function of Distance and Drift Tube Radius $R_c$ . . . . . 21
21. Radial Distribution of the Current Density of the Beam, Plasma, and Total Current Flow . . . . . 23
22. Photographs of Background Gas Glow . . . . . 24
23. Energy Spectrum Time Scan of a 1 MeV Maximum Energy IREB with a 37 kA Current Pulse at a 1 m Transport Distance at Different Background Pressures . . . . . 26
24. Beam Current Pulse Oscillograph Trace for IREB Transport in Air at a Distance of 1 Meter . . . . . 27
25. IREB Current Pulses at the End of the Drift Tube 0.8 m and 2 m at Various Background Gas Pressures . . . . . 28
26. Value of the Energy at the Maximum Current Peak $E_m$ as a Function of Pressure p and Transport Length L . . . . . 29
27. Pulse Length as a Function of Background Pressure and Transport Length, L . . . . . 30
28. Beam Current Density Radial Distribution at Different Times After Injection . . . . . 32
29. Distance to Off-Axis Displacement as a Function of Pressure . . . . . 33
30. Electron-Optical Converter Graphs of Axial Displacement . . 33
31. Beam Current Density Distribution as a Function of Time . . . . . 34
32. Oscillograms of the Voltage V, Diode Current I, and Beam Current Density $J_b$ as Measured with Sectioned Faraday Cups Located at Different Distances from the Chamber Axis . . . . . 35
33. Gas Density Radial Distribution at Different Times After Beam Injection . . . . . 38
34. Gas Density Along the Axis of the Beam as a Function of Time After the IREB Injection . . . . . 39
35. Maximum Amplitude of the Gas Compression Coordinate as a Function of Time After the Beam Injection for $j = 1\ kA/cm^2$ . . . . . 39
36. (a) Gas Density Radial Distribution Observed 34 $\mu$s After the IREB Pulse; (b) Radial Distribution of the Beam Energy Release into the Gas . . . . . 40
37. Dependence of the Gas Density Along the Beam Axis Upon Time . . . . . 41
38. Dependence of the Released Energy Density Along the Beam Axis Upon the Change in Gas Density at $t_{observed} \gg t_s$ . . . . . 41

39. (a) Total Beam Current as a Function of Distance from Injection at a Pressure of 75 Torr in He; (b) Total Beam Current as a Function of Pressure in He at a Distance of 113 cm from Injection . . . . . 43
40. Plasma Current to Beam Current Ratio as a Function of Gas Pressure . . . . . 44
41. Energy Carried by the Beam to Different Distances as a Function of Gas Pressure . . . . . 46
42. Energy Carried by the Beam as a Function of Distance for Various Gas Pressures . . . . . 47
43. Pressure Required for Maximum Energy Carried by the Beam to Different Distances . . . . . 47
44. Time Plots Showing the IREB Energy Spread at Three Locations Along the Drift Tube for p = 0.4 and 4 Torr . . . . 48
45. Beam Energy Spectra as a Function of Background Pressure at Two Transport Distances . . . . . 49
46. Specific Energy of the Transported Electron Beam at Different Transport Distances as a Function of Gas Pressure . . . . . 49
47. Dependence of the Microwave Radiation Intensity Upon Gas Pressure and Transport Length . . . . . 50
48. Dependence of the Soft X-ray Radiation Emanating from the Plasma Upon Background Gas . . . . . 51
49. Radial Distribution of Beam Current Density and IREB Particle Angle Distribution in the Drift Tube for Various Times and Pressures . . . . . 51
50. Beam Current Pulse Scan . . . . . 53
51. Dependence of System Parameters Upon Background Gas Pressure . . . . . 54
52. Apparatus for the Formation of Positively Charged Electron Beams Showing the Voltage Radial Distribution . . 58

# TABLES

1. Institutes Involved in Research on IREB Propagation Through Air . . . . . 2
2. Accelerators and Beam Parameters in the Experimental Research on IREB Propagation . . . . . 4

# GLOSSARY

The IREB and plasma channel parameters being considered by the Soviet researchers are as follows:

| *IREB Parameters* | *Symbol* | *Units* |
|---|---|---|
| Beam energy | $E_b$ | MeV, keV |
| Beam current | $I_b$ | kA |
| Beam current density | $J_b$ | $kA/cm^2$ |
| Beam radius | $r_b$ | cm |
| Beam radius (at input to drift tube) | $r_{bo}$ | cm |
| Azimuthal magnetic field | $B_\theta$ | G, kG |
| Time after pulse | t | $ns$, $\mu s$ |
| *Plasma Channel Parameters* | | |
| Background gas pressure | p | Torr |
| Optimum background gas pressure (for best IREB propagation) | $p_{opt}$ | Torr |
| Propagation length | z | m |
| Total length of drift tube | L | m |
| Gas or channel plasma electron density | $n_e$ | $cm^{-3}$ |
| Gas or channel plasma ion density | $n_i$ | $cm^{-3}$ |
| Characteristic plasma electron energy | $\epsilon_k$ | eV |
| Conductivity of plasma channel | $\sigma$ | $mho/m$ |
| Plasma current | $I_p$ | kA |
| Plasma current density | $J_p$ | $kA/cm^2$ |
| Reverse plasma current | $I_r$ | kA |
| Net total current | $I_T$ | kA |
| Drift tube inside radius | $R_c$ | cm |
| Plasma channel radius | $r_p$ | cm |
| Plasma magnetic field decay time | $\tau_d$ | ns |

# I. INTRODUCTION

Soviet research on the propagation of intense relativistic electron beams (IREB) through fairly high-pressure air (pressure range 0.1 to 760 Torr) since the early 1970s included the study of the plasma channel created by the passage of the electron beam through air, the resistive hose instability and its effect on beam propagation, the effect of self-fields, current enhancement, gas expansion, return currents, inherent beam energy spread, and other factors.

This report covers Soviet developments in IREB propagation through air where the beam is not focused by external magnetic fields. The information was obtained from Soviet open publications with emphasis given to the last ten years of beam propagation in the USSR. The background pressure of air considered here varies from 0.1 Torr to atmospheric pressure. Soviet work on IREB transport through air at low pressures (from $10^{-6}$ to $10^{-2}$ Torr) was considered in a previous report [1]. Earlier work on Soviet developments of IREB propagation through air can be found in an earlier RAND publication by Kassel and Hendricks [2].

Most Soviet beam propagation research has been carried out at nine institutes as shown in Table 1. Researchers and their leaders are listed under their institutes in the appendix. The chronology of the key Soviet research on IREB propagation through air is presented in Fig. 1 for the nine institutes and their leading researchers.

Figure 1 also indicates the extent, initiation, and termination of the specific research within the individual institutes. Note the short time span of the experimental research carried out by the Yu. P. Usov team at IYaF-TPI where many researchers apparently made a concentrated effort, and the similar short and limited effort made at NIIEFA and NIITP but with no recent publications. Also of interest is the large effort carried out by two teams at KhFTI, with a complete cutoff in publications in 1981 and 1982, respectively. With the termination of publication on these five important experimental investigations comes the onset of five research efforts that are currently represented by recent publications in IYaF-TPI (Team 1: V. P. Grigor'yev), IAE (L. I. Rudakov), FIAN-IOF (A. A. Rukhadze), VEI (A. V. Zharinov, M. A. Vlasov), and MFTI (K. V. Khodatayev).

Seven of the abovementioned institutes carried out experimental investigations on IREB propagation through air. Table 2 shows the accelerators used in this research, together with the beam and propagation parameters.

Table 1

INSTITUTES INVOLVED IN RESEARCH ON IREB PROPAGATION THROUGH AIR

| | Name | Acronym | Location | Type of Research | Area of Research |
|---|---|---|---|---|---|
| 1. | Institute of Nuclear Physics Research of the Tomsk Polytechnical Institute | IYaF-TPI | Tomsk | Theoretical computer simulation and experimental | Electron beam and plasma channel properties |
| 2. | The Institute of Atomic Energy (Kurchatov) | IAE | Moscow | Experimental and theoretical | Formation of the resistive hose instability |
| 3. | The Lebedev Physics Institute together with The Institute of General Physics | FIAN<br>IOF | Moscow<br>Moscow | Experimental | Beam current enhancement, IREB thermal effects and their perturbance upon the background gas density |
| 4. | The Physico-technical Institute of Kharkov | KhFTI | Kharkov | Experimental | Electron beam and background gas properties for optimum beam propagation |
| 5. | The Yefremov Institute of Electrophysical Equipment | NIIEFA | Leningrad | Experimental | Return current enhancement and two-stream instability limitations at the lower pressure limit |
| 6. | The Scientific Research Center of Thermal Processes | NIITP | Moscow | Experimental | Injection of an electron beam into atmospheric pressure air through an elaborate differential pumping system |
| 7. | The All-Union Electrical Engineering Institute | VEI | Moscow | Theoretical and experimental | Electron beam properties, gas expansion, and the injection of IREBs through gas gradients such as differential pumping systems |
| 8. | The Moscow Physico-Technical Institute | MFTI | Moscow | Theoretical | Formation of the resistive hose instability |
| 9. | Institute of Experimental Meteorology | IEM | Obninsk | Theoretical | Self-channeling of electron beams |

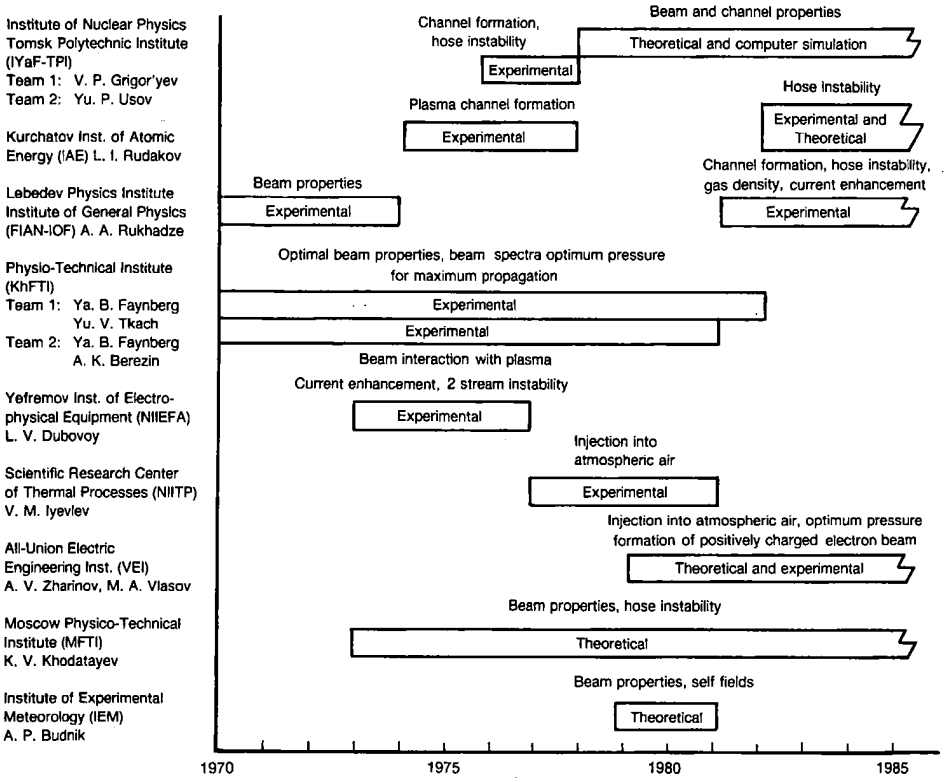


Fig. 1—Chronology of Soviet research on IREB propagation through air (pressure from 0.1 to 760 Torr)

Table 2

ACCELERATORS AND BEAM PARAMETERS IN THE EXPERIMENTAL RESEARCH ON IREB PROPAGATION

| Institute | Accelerator | Beam Energy | Parameters of Beam Current | Pulse Length | Beam Radius | Pressure Range | Optimum Propagation Pressure | Propagation Distance |
|---|---|---|---|---|---|---|---|---|
| IYaF-TPI, Tomsk | Tonus | 1 MeV | 35–40 kA | 60 ns | 2 cm | 0.1 to 100 Torr | 0.1 to 0.6 Torr | 1 to 2 m |
| IAE (Kurchatov) Moscow | Neptun | 450 keV | 20kA | 60 ns | 1 to 3 cm | 1 to 100 Torr | 1 Torr | 3 cm to 3 m |
| IOF-FIAN (Lebedev) Moscow | Terek-IR | 1.5 MeV | 4–25 kA | 60 ns | 1.5 to 3 cm | 1 to 750 Torr | 1 Torr | to 1.2 m |
| KhFTI, Kharkov | Kharkov | 1 MeV | 50 kA | 40 ns | 1.6 to 1.8 cm | 0.1 to 100 Torr | 1 Torr | to 3 m |
| | Linear Accel. | 2 MeV | 1A | 2 $\mu$s | 1 cm | 760 Torr | | 0.6 m |
| | LU-40 (Lin Accel. | 20 MeV | 0.5A | 10 $\mu$s | 1 cm | | | to 2 m |
| NIIEFA, Leningrad | REP-5 | 1.5 MeV | 50 kA | 20 ns | 0.6 cm | $10^{-3}$ to 40 Torr | $10^{-2}$ to 1 Torr | to 1.2 m |
| NIITP, Moscow | | 500 keV | cw | | | 760 Torr | | 0.3 m |
| VEI, Moscow | | 300 keV | 20–27A | 400–500 $\mu$s | 0.3 cm | 0.1 to 400 Torr | | |

The experimental research carried out in the first five institutes shown in Table 2 utilized IREBs with energies of 0.5 to 1.5 MeV, beam currents of 15 to 50 kA, and pulse lengths of 20 to 60 ns, with beam propagation lengths from fractions of a meter to three meters. In the case of the KhFTI research, two experiments are included where higher beam energies were used but at low beam currents.

Theoretical work of any consequence was carried out only at IYaF-TPI, MFTI, and in a very limited way at VEI. Out of the seven institutes that have performed experiments, only IYaF-TPI has carried out computer simulation work of any magnitude. The theoretical work at MFTI is somewhat of a mystery, the papers not being clear on applications and analysis. However, the researchers at MFTI under Khodatayev's leadership are of interest, and their citations refer to many U.S. researchers working on IREB propagation.

Figure 2 (a and b) plots the total number of Soviet open source papers published specifically on research of IREB propagation through and injection into air for the past 15 years, and the number of authors of these papers. The research papers on the use of IREBs for optical pumping, beam welding, and other electron beam applications that are not obvious for beam transport are not included. The number of papers as a function of years gradually increases with distinct peaks during 1974, 1978, 1981, and 1984. The great jump of activity in 1984 demonstrates an increase of more than a factor of three of papers published in 1984 over the number published in 1983.

The plot of number of authors publishing the research papers is a demonstration of relative effort. Each author was considered to be active (and was therefore counted) a year before the date of his first published paper until one year after his last published paper. Figure 2b demonstrates a sharp increase in the number of authors involved in the IREB transport research from 1980 to 1984.

This abrupt jump in the number of publications and authors participating in the research in 1984 may signify an increase in the recent overall Soviet effort on IREB transport through air, but it may also be the result of a Soviet declassification of earlier research, which is only now able to be published. The peak may therefore represent the "dumping" of papers.

The existence of an active Soviet CPBW program cannot be directly inferred from the available data as presented in the Soviet open source literature because of the low energies (of 1.5 MeV and below) and beam propagation distances (of 3 meters or less) used in the experiments. The Soviet work, however, does demonstrate a broad research effort, involving some key elements of IREB propagation through the air. The sharp increase in published Soviet papers in recent years implies a significant increase in the research effort in this area.

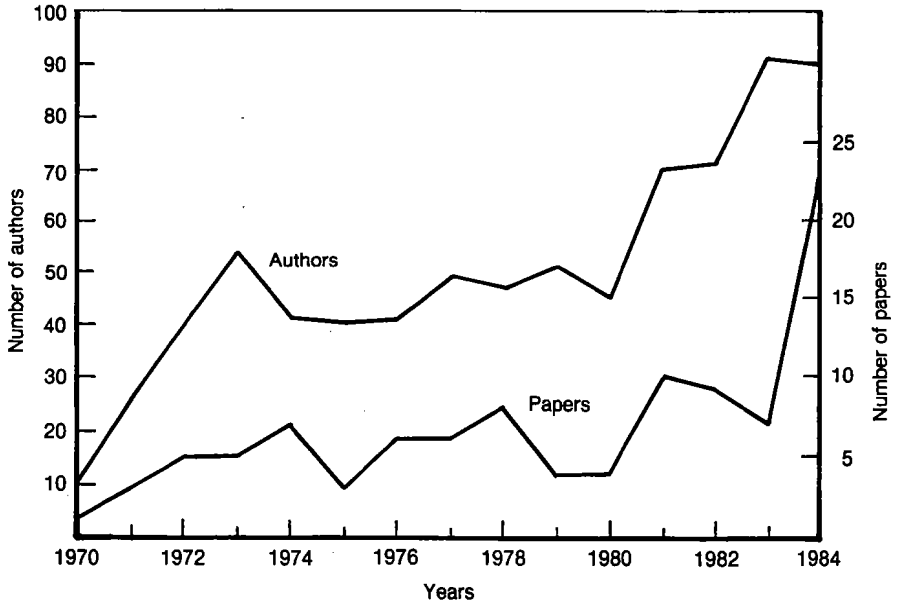


Fig. 2—Number of Soviet open source papers (lower curve) published on IREB propagation through air, and the number of authors of these papers (upper curve) as a function of years

# II. IYAF-TPI RESEARCH

## THEORY AND COMPUTER SIMULATION

Propagation research of the Nuclear Physics Institute attached to the Tomsk Polytechnical Institute (IYaF-TPI) has been performed by two separate research teams. The first, headed by V. P. Grigor'yev, carried out theoretical calculations and computer simulation studies of IREB propagation from 1977 to the present. The second team, headed by Yu. P. Usov, performed several experiments with IREB propagation, described in the next subsection.

In 1979–1980 the theoretical team carried out computer simulation studies using the BESM-6 computer to investigate plasma channels formed by the injection of IREBs into air and neutral gas at pressures in the range of 1 to 100 Torr. The team considered plasma channel inhomogeneities along the beam axis, the effect of the $B_z$ field gradient along the axis and its effect upon beam radius, and beam current neutralization in the plasma channel for beam pulse lengths of 10 to 80 nsec. For these calculations the researchers took the values of the beam parameters from early transport experiments using the "Tonus" accelerator with a beam energy of 1 MeV and beam currents of 20 to 30 kA [3].

The computer simulation studies as carried out in 1979–1980 and described in Refs. 4 and 5 did not take into account the changes in charges and electron beam current distribution within the beam during IREB transport. The data and its discussion as presented in Figs. 3 through 12 are based on the simpler models, which are applicable only at low background air pressures and short beam transport distances and have been investigated in the pressure range from 0.2 to 40 Torr. Computer simulation investigations carried out in 1983 as described in Ref. 6 presented a more sophisticated model taking into account the beam's charge and current distribution. These more recent data are presented in Figs. 13 through 20 and were determined in the background air pressure range from 1 to 100 Torr.

The parameters involved in the above computer simulations were: the beam current, $I_b$; total system current $I_T$ [$I_T = I_b + I_p$, where $I_p$ is the plasma current]; beam current density, $J_b$; the azimuthal magnetic field $B_\theta$, beam radius, $r_b$; electron plasma density, $n_e$; characteristic energy of plasma electrons $\epsilon_k$; and the conductivity of the plasma channel, $\sigma$, as functions of background gas pressure, p; propagation length, $z$; time after the pulse, $t$; beam radius, $r_b$; and drift tube inside radius, $R_c$. (See the Glossary for symbol definitions.)

The variation of $B_\theta$ and $I_T$ along the beam axis for background air pressures of 1 and 10 Torr are shown in Fig. 3, and the axial variation of $B_\theta$ as a function of $p$ is shown in Fig. 4. The radial $B_\theta$ field distribution for a background pressure of 1 Torr is shown in Fig. 5 [4].

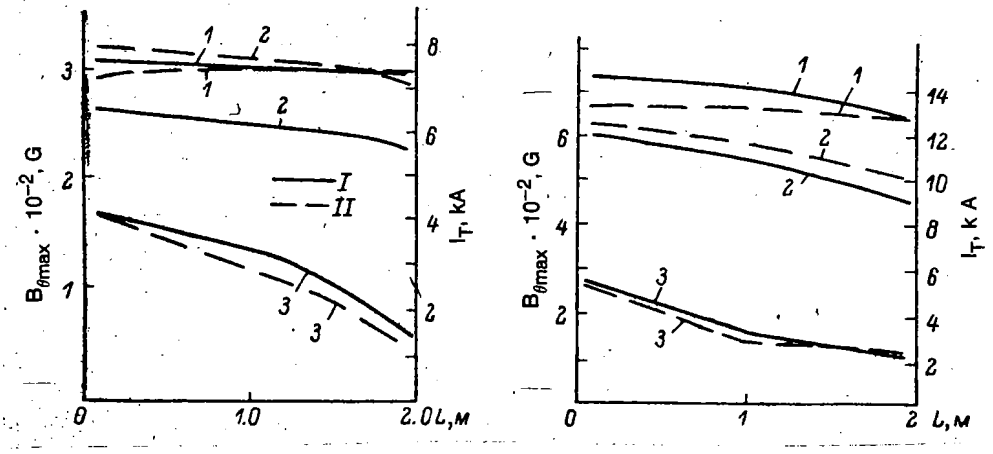


Fig. 3—Axial profile of the azimuthal magnetic field $B_\theta$(solid lines) and the total current $I_T$ (dashed lines) for p = 1 and 10 Torr for times t = 50 ns – curve 1, 30 ns – curve 2, and 10 ns – curve 3 [4]

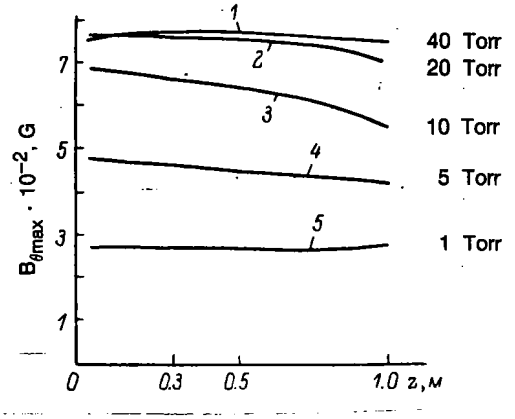


Fig. 4—Axial profile of the azimuthal magnetic field $B_\theta$ in a 1 meter long drift tube, t = 30 ns [4]

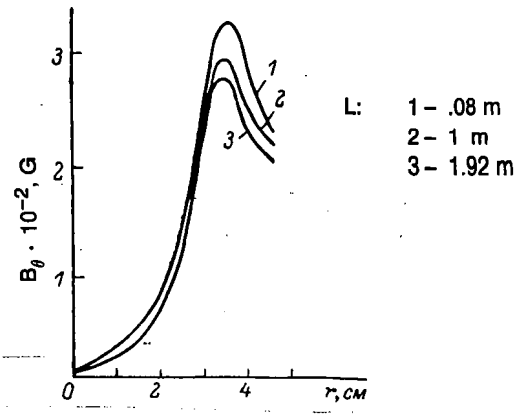


Fig. 5—Radial $B_\theta$ field distribution for p = 1 Torr, t = 20 ns as a function of various axial distances [4]

Soviet theory points out that the decrease in $B_\theta$ indicates a noticeably defocusing condition of the beam at $t \geq 30$ *ns*; but at short beam transport distances, the basic structure of the electron beam does not change even at the high air pressure of 40 Torr.

As seen in Fig. 5, the magnetic field intensity is located in a narrow band at the edge of the beam with the area in the middle of the beam practically magnetically neutralized. This $B_\theta$ field radial distribution is the same for other background pressures, except that the degree of magnetic neutralization in the center of the beam decreases with an increase in pressure (as seen in Fig. 4).

The longitudinal profiles of the plasma density in the plasma channel at different pressures are shown in Fig. 6. The azimuthal magnetic

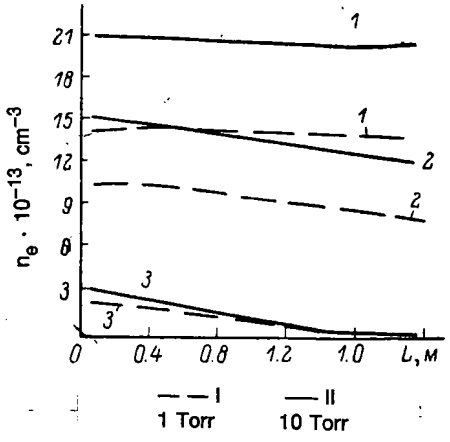


Fig. 6—Plasma density longitudinal profile at p = 1 Torr (dashed line) and 10 Torr (solid line) at times of: t = 50 (1), 30 (2), and 10 ns (3) [4]

field $B_\theta$ decreases along the beam path for IREB transport over distances greater than 1 meter in the pressure range > 10 Torr. Such a $B_\theta$ gradient demonstrates a significant erosion of the beam front. This effect, however, can find an application in shortening the beam pulse. The simulation also showed that the radius of the plasma channel can be considerably larger than the beam radius at pressures below 1 Torr. At higher pressures the radii of the beam and plasma channel are practically the same. The beam current density radial distribution as a function of pressure is shown in Fig. 7 [5].

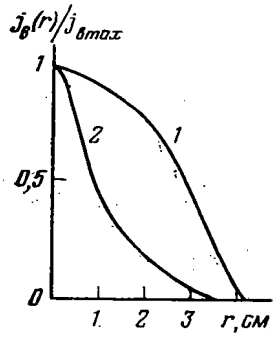


1 — p = 1, 10 Torr
2 — p = 0.2, 0.5 Torr

Fig. 7—Radial distribution of the beam current density for several background air pressures [5]

The measured and calculated values of the total beam current pulses are shown in Fig. 8 for a $z = 30cm$ [5]. Experimental values of the total current are shown by dashed lines demonstrating good agreement between experiment and theory for these cases.

The time dependence of the plasma density created by the transport of the electron beam through a 12 cm radius drift tube for different pressures is shown in Fig. 9 [5]. The plasma density produced from the collision and cumulative ionization in the area of the beam ($r = 0$) increases rapidly and reaches a maximum value of about $3 \times 10^{14}\ cm^{-3}$ at a pressure of 10 Torr and $2 \times 10^{14}\ cm^{-3}$ at a pressure of 0.2 Torr.

Outside the electron beam the plasma density increases only by cumulative ionization processes and is strongly dependent upon the background gas pressure increasing by more than two tens for a decrease in pressure from 10 to 0.2 Torr. The plasma density within the beam in the pressure range of from 0.2 to 10 Torr was weakly dependent upon pressure and mainly dependent upon beam electron density.

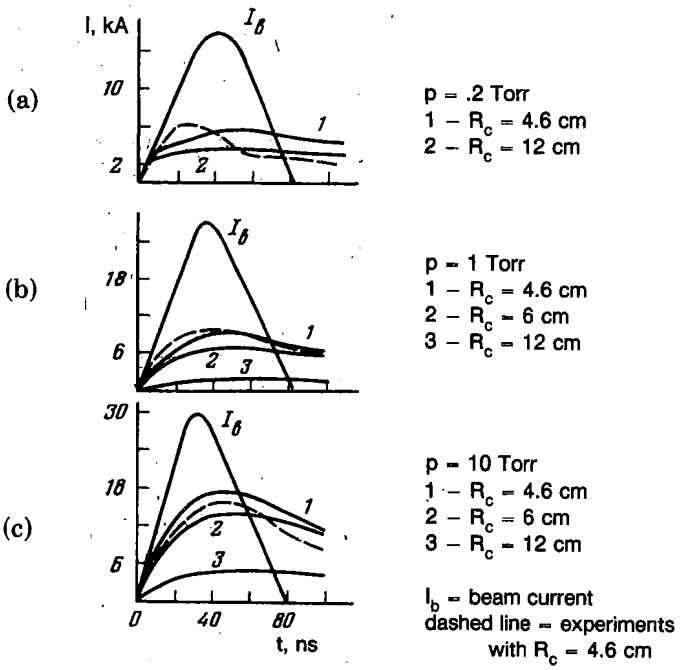


Fig. 8—Total beam current pulse as a function of background pressure and drift tube radius $R_c$ [5]

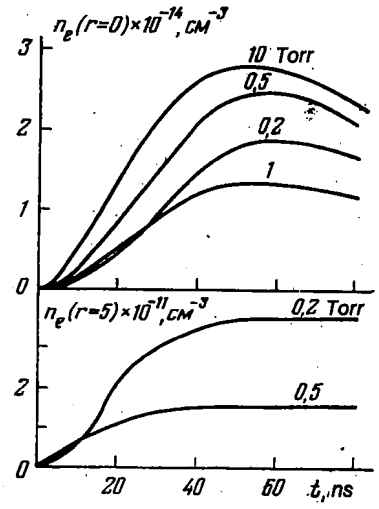


Fig. 9—Time dependence of the plasma density ($n_e$) as a function of background pressure for r = 0 and r = 5 cm [5]

The radial distribution of the plasma density as a function of several pressures and several beam drift tube radii is shown in Fig. 10. In the 0.2 to 10 Torr pressure range, the plasma density follows the radial

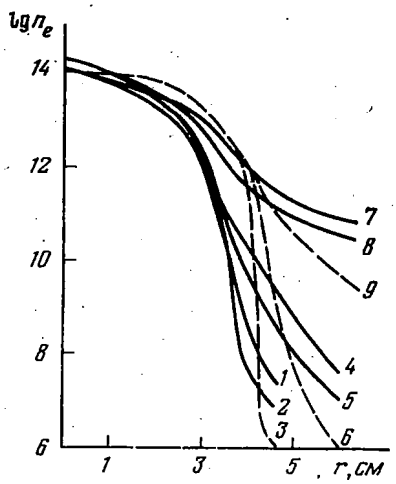


$R_c$ = 4.6 cm, 1 – p = 0.2 Torr, 2 – 0.5 Torr, 3 – 1 Torr
$R_c$ = 6 cm, 4 – p = 0.2 Torr, 5 – 0.5 Torr, 6 – 1 Torr
$R_c$ = 12 cm, 7 – p = 0.2 Torr, 8 – 0.5 Torr, 9 – 1 Torr

Fig. 10—Radial plasma density distribution ($n_e$) as a function of background pressure and drift tube size for a time of 37 ns after initiation of the beam pulse [5]

profile of the beam density, depends weakly upon pressure, and falls off rapidly beyond the beam with increased background pressure. The radial plasma density distribution was flat at the beam axis and steep at the beam edge. The dependence of the plasma channel radius upon pressure for several drift tube radii is shown in Fig. 11.

The characteristic plasma electron energy ($\epsilon_k$) averaged over the beam cross section, as a function of time for various background pressures, is represented in Fig. 12a. The radial distribution of the plasma electron energy is shown in Fig. 12b for the various background pressures. Figure 12a shows that $\epsilon_k$ has a maximum at the start of the beam current pulse when the fields produced at the beam front are large and then it decreases with time. In the radial distribution of $\epsilon_k$ (Fig. 12b) the value of $\epsilon_k$ in the area of the electron beam remains fairly constant and falls off slowly with increasing radial distance. The value of $\epsilon_k$ decreases with increasing background pressure, which is due

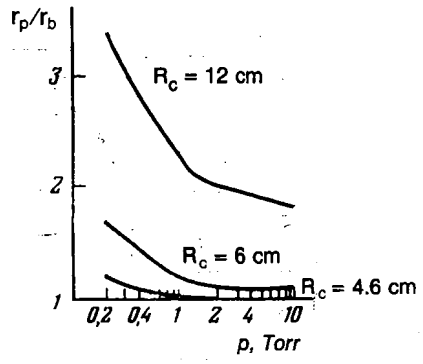


Fig. 11—Plasma channel radius $r_p$ as a function of background pressure for several drift tube radii [5]

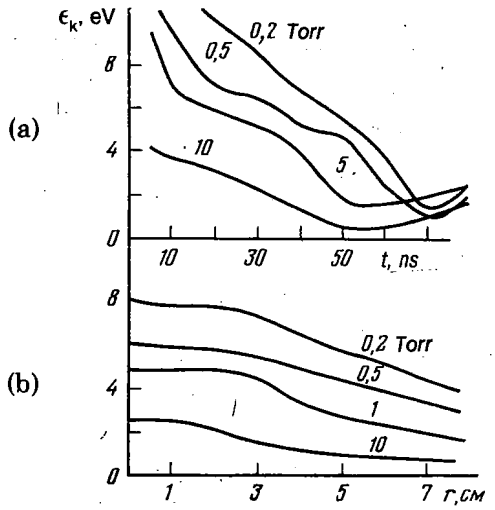


Fig. 12—Characteristic average plasma electron energy ($\epsilon_k$) as a function of time (a) and its radial distribution (b) at time t = 37 ns and drift tube radius of 12 cm for various background pressures [5]

to the increase of the collision frequency $\nu_{em}$ of the plasma electrons with the gas molecules as the pressure increases. The plasma electrons lose their energy with each collision in time $1/\nu_{em}$ and do not have enough time to obtain a high energy.

The beam was found to induce a current flowing opposite to the direction of the electron beam in the plasma. Most of this current flows within the electron beam; and its current density, $J_p$, was found to decrease rapidly with increasing radius.

The IYaF-TPI researchers state that they are quite satisfied with the mathematical model as presented in Refs. 5 and 7 that demonstrated good agreement between experiment and theory in the pressure range of 0.2 to 10 Torr. The investigators determined an optimum beam neutralization at the pressure of about 1 Torr and found that it is very dependent upon the inner radius of the metal tube. They found that this optimum beam neutralization increases with an increase in drift tube radius.

The theoretical models of Refs. 4 and 5 allowed the IYaF-TPI researchers to narrow the gap between theory and experiment. However, in these models the beam characteristics were predetermined and the change in charge and current distributions within the beam were not taken into account in the process of beam transport. These assumptions, as was shown in the experiments of Refs. 3 and 7, are correct only in the case of low pressures and short distances, because at higher background gas pressures and larger beam transport distances, the beam current and charge density profiles change, which leads, in turn, to a change in the plasma channel parameters. Another model for use at higher pressure and longer transport distances was proposed in 1983 in Ref. 6, taking into account the change in the parameters of the plasma channel formed by the IREB and the changes in beam charge and current density profiles.

A numerical simulation, made in Ref. 6, assumed an IREB through air at pressures from 1 to 100 Torr, with the electron energy in tens of eV inside the plasma channel, and approximating the recombination coefficient by the Mehr and Biondi formula [8]. The plasma density $n_e$ as a function of transport distance and time is shown in Figs. 13 and 14, respectively [6].

The plasma density was seen to reach $4.5 \times 10^{15}\ cm^{-3}$ in 30 ns at pressures 50 to 70 Torr and about $2.5 \times 10^{15}\ cm^{-3}$ at pressures from 1 to 20 Torr. Beyond 30 ns the plasma density decreased because the recombination rate (mostly dissociative) was greater than the ionization rate. The plasma channel radius at pressures greater than 1 Torr coincided with the beam radius, and the radial profile $n_e(r,z,t)$ was very close to $n_b(r,z,t)$. The plasma channel was inhomogeneous along

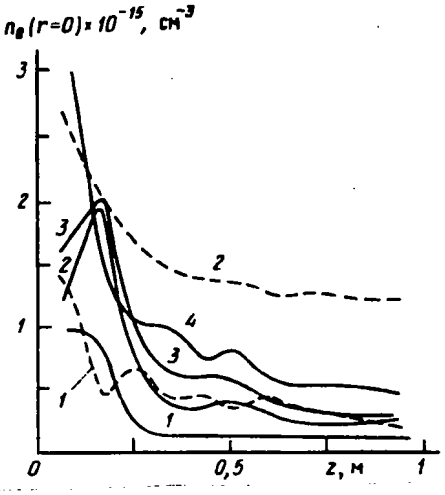


Dashed lines represent a pressure of 1 Torr
1 – t = 10 ns 2 – t = 40 ns
Solid lines represent a pressure of 20 Torr
1 – t = 6 ns 2 – t = 10 ns
3 – t = 17 ns 4 – t = 40 ns
where $r_{bo}$ is the beam radius at the entrance to the drift tube and $R_c$ is the drift tube radius

Fig. 13—The plasma electron density ($n_e$) distribution along the drift tube with $r_{bo}$ = 1 cm, $R_c$ = 2 cm [6]

the length of the drift tube, especially at the higher pressures and for large initial beam densities.

The dependence of the density of the plasma in the channel upon gas pressure and initial beam current density was found to be complex, because of all these factors affecting beam density and ionization rate. At short distances from the point of beam injection the plasma electron density $n_e$ was greater at higher gas pressures. The $n_e$ dependence was different at the output of the drift tube, however. For $t < 10$ to 12 ns, $n_e$ was lower at $p$ = 1 Torr than at $p$ = 10 to 100 Torr. However, for $t > 12$ *ns*, $n_e$ increased more rapidly at $p$ = 1 Torr.

The characteristic energy of the plasma electrons ($\epsilon_k$) was found to depend only weakly upon the gas pressure. The value of $\epsilon_k$ was found to vary from 1 to 14 eV over this pressure range and along the whole length of the channel. The higher values of $\epsilon_k$ (5 to 14 eV) were found for $p$ = 1 Torr and the lower values (0.5 to 2 eV) for $p$ = 100 Torr. The value of $\epsilon_k$ was found to be very weakly dependent upon the

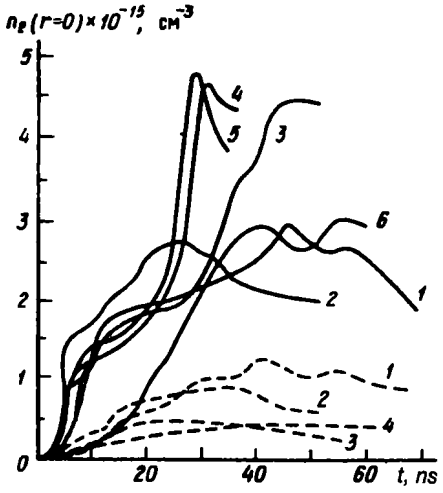


Solid lines represent Z = 8 cm, with pressures of:
1 – 1 Torr 2 – 10 Torr 3 – 20 Torr
4 – 50 Torr 5 – 70 Torr
with $r_{bo}$ = 1 cm, $R_c$ = 6 cm
6 – 20 Torr, $r_{bo}$ = 3 cm, $R_c$ = 6 cm
Dashed lines represent Z = 92 cm, with pressures of:
1 – 1 Torr 2 – 10 Torr 3 – 20 to 70 Torr
with $r_{bo}$ = 1 cm, $R_c$ = 2 cm
4 – 20 Torr, $r_{bo}$ = 3 cm, $R_c$ = 6 cm

Fig. 14—Dependence of $n_e$ upon time [6]

radius. This can also be seen in Fig. 12 with earlier calculations of $\epsilon_k$ as a function of $r$ and $t$ [5].

The plasma channel conductivity ($\sigma$) was found to have a strong dependence upon gas pressure and at pressures greater than 1 Torr was determined totally by plasma electron collisions with neutrals. This $\sigma$ depends not only upon $\epsilon_k$ but also upon the ratio of the densities of the plasma and neutral molecules. The conductivity was thus found to decrease rapidly with an increase in gas pressure, and its radial distribution is similar to that of the $n_e$ distribution. The dependence of $\epsilon_k$ and $\sigma$ upon gas pressure is demonstrated in Fig. 15.

The simulation of the total current $I_T = I_b + I_p$ and the azimuthal magnetic field $B_\theta$ demonstrates that the basic plasma current flows in the area of the axis of the beam and decreases as $r$ approaches $r_b$. With increase in gas pressure and because of the decrease in the plasma channel conductivity, the current neutralization weakens and

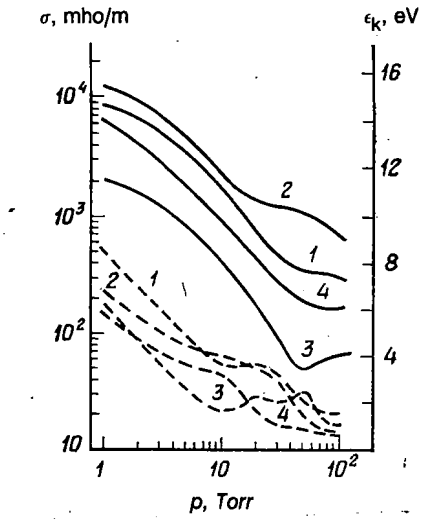


Solid curves represent $\sigma$ and dashed curves represent $\epsilon_k$
1 – t = 10 ns, z = 8 cm
2 – t = 33 ns, z = 8 cm
3 – t = 10 ns, z = 92 cm
4 – t = 33 ns, z = 92 cm

Fig. 15—Dependence of the characteristic energy of the plasma electrons ($\epsilon_k$) and the conductivity of the plasma channel ($\sigma$) upon gas pressure (p) for r = 0, $r_{bo}$ = 1 cm, $R_c$ = 2 cm [6]

$B_\theta$ grows near the point of beam injection. The radial distribution of current neutralization becomes more homogeneous. The $B_\theta$ radial distribution found in Ref. 6 is similar to the earlier findings made in Refs. 4 and 5. According to Ref. 6, $B_\theta$ increases with time, and the sharp dependence of $B_\theta$ as a function of $z$ is seen only at the beginning of the drift tube. At the end of the tube the dependence on $t$ becomes insignificant, as demonstrated in Fig. 16.

In the light of the above theoretical results, the IYaF-TPI researchers explain electron beam focusing as follows: A drift of plasma electrons is observed along the beam radius as a result of the movement of the electron beam in the $B_\theta$, which increases in time and falls off with distance. Because $B_\theta$ increases with time, the electrons obtain a velocity directed toward the beam axis, and because of the $B_\theta$ gradient along $z$, the velocity is directed along the axis. Beam electrons follow trajectories that are oscillations with either decreasing or increasing radial amplitudes, depending upon which forces of the magnetic field predominate. Thus the beam either focuses or defocuses.

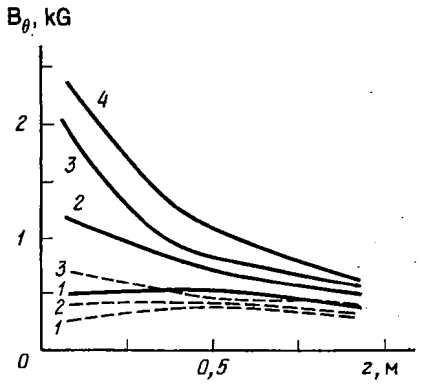


Dashed curves: p = 1 Torr
1 – t = 7 ns
2 – t = 17 ns
3 – t = 33 ns
Solid curves: p = 50 Torr
1 – t = 6 ns
2 – t = 10 ns
3 – t = 17 ns
4 – t = 33 ns

Fig. 16—Axial profile of the azimuthal magnetic field $B_\theta$ for $r = r_{bo}$ = 1 cm, $R_c$ = 2 cm [6]

The beam dynamics calculations are shown in Figs. 17–19 [6]. In Fig. 17, curve 1 represents the beam pulse without any current loss at the output with the following two conditions:

$p$ = 1 Torr, $r_{bo}$ = 1 cm, $R_c$ = 2 cm

$p$ = 20 Torr, $r_{bo}$ = 3 cm, $R_c$ = 6 cm

Figure 17 indicates that a beam having a high current density of about 7.6 kA/cm$^2$ at the input to the drift tube can be transported without losses only for pressures less than 5 Torr. At higher pressures, only the leading edge of the beam pulse can pass, while the trailing edge is cut off. This shortens the pulse and decreases its amplitude at the drift tube output. The cutoff effect is more evident at higher gas pressures and beam current densities, in longer drift tubes, and with smaller tube radii. As an example, beam transport was computed for beam pulse increasing from $I_{b\,max}(z = 0)$ = 23.7 kA, $J_{bo}$ = 7.6 kA/cm$^2$ to $I_{b\,max}$ ($z$ = 0) = 50 kA, $J_{bo}$ = 16 kA/cm$^2$. Pulse length was found to decrease from 33 to 26 ns for $L$ = 1 m, $R_c$ = 2 cm. The

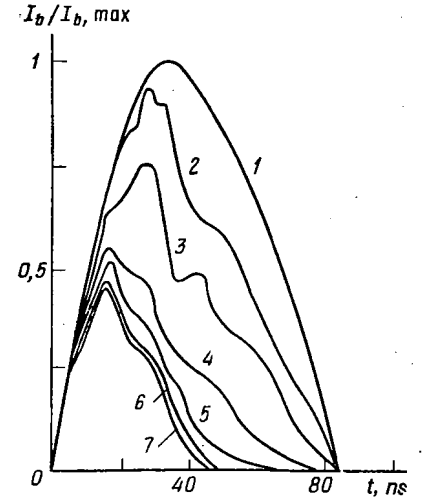


1 – at the input to the drift tube
2 – 7 at the output of the drift tube
2 – p = 5 Torr
3 – p = 10 Torr
4 – p = 20 Torr
5 – p = 30 Torr
6 – p = 50 Torr
7 – p = 70 to 100 Torr
with $I_{b\,max}$ = 23.7 kA, $r_{bo}$ = 1 cm, $R_c$ = 2 cm

Fig. 17—Electron beam current pulse shape [6]

ratios of the beam current values at the input and output of the drift tube were 0.56 and 0.38, respectively.

The above theoretical results were in good agreement with experiments performed in 1967 [9] when it was determined that current was cut off at the trailing edge of the pulse in drift tubes 1 meter long at pressures above 6 Torr.

Figure 17 indicates that the current cutoff stabilized at pressures from 50 to 70 Torr, and there was no further pulse shortening beyond 70 Torr. There also was no current cutoff at pressures below 5 Torr. Both effects were attributed to current neutralization. At low pressures, the gradient of the axial magnetic field is flattened out (see Fig. 16); and therefore there is no pulse current cutoff present. The conductivity of the plasma channel is then high enough (Fig. 15) and the level of current neutralization is also sufficiently high during the entire pulse. As pressure increased beyond 5 Torr, plasma channel conduc-

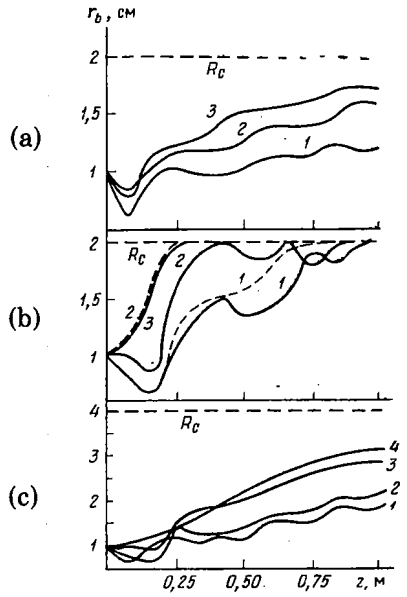


(a) p = 1 Torr: 1 – t = 10 ns, 2 – t = 33 ns, 3 – t = 65 ns
(b) solid curves – p = 50 Torr: 1 – t = 10 ns, 2 – t = 17 ns, 3 – t = 33 ns
dashed curves – p = 70 to 100 Torr: 1 – t = 10 ns, 2 – t = 33 ns
(c) p = 20 Torr: 1 – t = 10 ns, 2 – t = 17 ns, 3 – t = 33 ns, 4 – t = 65 ns

Fig. 18—Dependence of the beam radius $r_b$ upon the axial length z [6]

tivity decreased (Fig. 15); and the level of current neutralization was no longer sufficient to flatten out the $B_\theta$ field gradient and to ensure the beam transport without loss. Above 50 Torr, the conductivity of the channel decreased to such an extent that plasma current had practically no effect upon the axial magnetic field distribution. $B_\theta$ was then determined only by the inhomogeneity of the injected beam at the beam front and by its current density change in the process of beam transport.

The change in beam parameters along the drift tube is shown in Figs. 18 and 19. At short distances from the beam injection plane ($z \sim 8$ to 16 cm), the beam was focused by a sharp increase of $B_\theta$ in time. As the beam traveled further, it started spreading; and the basic electron losses occurred at $z \geq L/2$. At the end of the drift tube, at pressures greater than 10 Torr and $T > 18$ ns, the electron beam den-

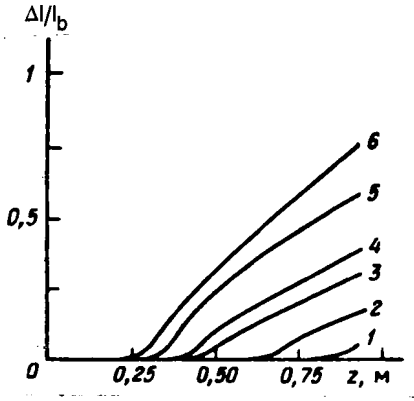


$R_c$ = 2 cm, p = 50 Torr
1 – t = 10 ns, 2 – t = 14 ns, 3 – t = 17 ns,
4 – t = 20 ns, 5 – t = 26 ns, 6 – t = 33 ns

Fig. 19—Relative beam current losses for $r_{bo}$ = 1 cm [6]

sity on axis sharply dropped, and the radial beam profile $n_b(r)$ was homogeneous along the entire cross section of the drift tube. Beam spreading decreased with increasing drift tube radius $R_c$ (Fig. 20). This can be attributed to the increase of the inductance of the system with increasing $R_c$ and the increase in current neutralization.

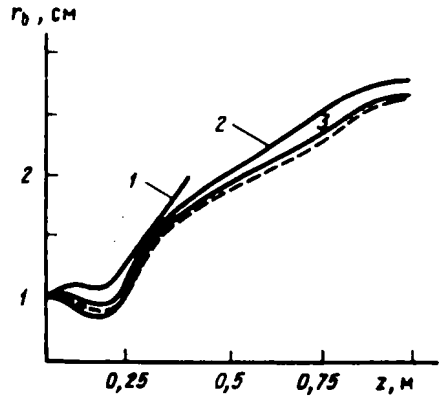


1 – $R_c$ = 2 cm, 2 – $R_c$ = 4 cm, 3 – $R_c$ = 10 cm
dashed line – $R_c$ = 20 cm

Fig. 20—Beam radius $r_b$ as a function of distance and drift tube radius $R_c$ [6]

Soviet researchers stress that even dense electron beams have little beam loss at short distances from the beam injection plane up to pressures above 50 Torr (Fig. 19). A detailed analysis of the propagation of an IREB along a plasma channel with a return current (current flowing opposite to the IREB in the channel) was made in Ref. 10. Here the radial distribution of the charge density and currents of the electron beam, plasma electrons, and ions have been determined for the beam radius smaller than, equal to, and larger than the radius of the plasma channel.

The beam is assumed to be in equilibrium, with its space charge partially neutralized by the background gas ions. This steady state condition is possible when an IREB in injected into low-density plasma (where $n_b$ is the density of the electron beam and $n_i$ is the density of ions of the background gas). However, when the electron beam is injected into a dense plasma, space charge neutralization is also accompanied by a partial beam current neutralization, characterized by plasma electrons flowing opposite to the direction of the electron beam.

The duration of the return plasma current flow was found to be 0.1 microseconds for $r_b \sim 1$cm, $n_e \sim 10^{14}$ to $10^{15}$, and electron plasma temperature of $\sim 1$ eV and is longer than the usual beam current pulse length [10]. As a result, when Soviet researchers considered the equilibrium condition of electron beam transport, they found it necessary to take into account this plasma electron current as well as the effect of the background gas ions.

The radial potential distribution as a function of the system configuration, the electron beam radius, the plasma radius, and the total beam current have been investigated using the equations developed in Ref. 10. A specific calculation was made for the case when the electron and ion plasma radii were the same ($r_i = r_e = r_p$) and when the IREB radius was equal to the plasma radius ($r_b = r_p$).

With a net negative charge excess along the beam axis, the beam and plasma electron density increased to the outer beam periphery while the ion density decreased [10]. However, with a net positive charge excess along the axis, the beam and plasma electron density decreased to the beam periphery, while ion density increased. When the electron beam current density on the axis was greater than the plasma electron current density, the electron beam current density increased with an increase in beam radius while the plasma current density decreased. Thus, the radial distribution of the total current density of the system represented a hollow beam (Fig. 21a), which was in agreement with the 1971 experiments with IREB injection into dense plasma [11]. The current transported by the ions could be neglected in that case.

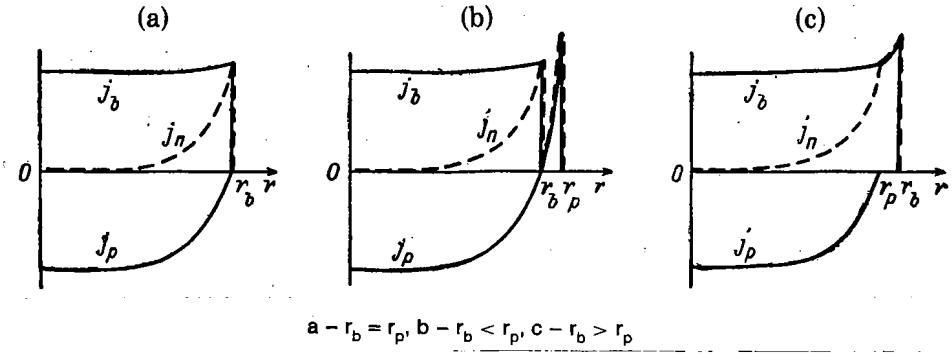


Fig. 21—Radial distribution of the current density of the beam, plasma, and total current flow [10]

When the IREB radius was smaller than the plasma radius ($r_p > r_b$), the current density of plasma electrons dropped to zero; with increasing radius and changing direction, it increased monotonically as it approached the plasma channel boundary (Fig. 21b). The radial profile of the total current in this configuration formed a double wall tube.

A beam radius can be larger than a plasma radius ($r_b > r_p$) when the beam is transported along thin metal wires or along a thin laser beam. The electron beam current density was found in this case to increase slightly to the plasma boundary; beyond it increased more rapidly to the beam boundary as shown in Fig. 21c.

The Soviet researchers state that IREB propagation in plasma with return current permits effective beam transport with beam currents that are considerably higher than those in static cases of neutralized electron beams. These beams have an application where it is necessary to create IREB with very high currents [10].

## IYAF-TPI RESEARCH—EXPERIMENTS ON CHANNEL FORMATION AND HOSE INSTABILITIES

The IYaF-TPI experimental research team headed by Yu. P. Usov performed several experiments in 1975–1977 involving plasma channels induced by IREB, hose instability, the optimal background pressure for IREB propagation, and the energy spread of beam electrons. These experiments were carried out using the Tonus accelerator operating at 1 MeV with beam currents from 35 to 40 kA, and a pulse length of 60 ns. No publications by this team were found after 1977.

The formation of the plasma channel was first observed by Soviet researchers in 1972 when an IREB was injected into air and gases at

pressures from 1 to 760 Torr [12]. In 1977, IYaF-TPI researchers demonstrated experimentally that the radius of the plasma channel created by an IREB was greater than the beam radius in the pressure range of 0.1 to 1 Torr, and the difference between the channel and beam radii increased with a decrease in pressure [13]. The same Tonus accelerator was used with a 4 cm diameter beam injected into a 9 cm diameter drift tube 60 cm long. Beam transport was found to be most effective in the pressure range of 0.09 to 0.06 Torr; however, long wave hose instabilities were observed in this pressure range with lateral beam displacement of the order of one beam diameter (Fig. 22a).

With further increase in background pressure, beam refocusing increased in these experiments because of increased current neutralization. In the pressure range for optimum beam transport, a glowing cylindrical layer appeared around the periphery of the beam (Fig. 22b). This layer was assumed to be a plasma channel carrying part of the return current of the beam. The channel was found to narrow down with increased pressure; and when the beam developed hose instability, the cylindrical symmetry of the layer was not disturbed but the whole beam was simply displaced laterally. Measurements revealed that no high energy electrons moving parallel to the beam flow were present in this layer region. From the analysis of data obtained in Refs. 3, 13, and 14, the IYaF-TPI researchers deduced that an IREB can be transported in large volumes, in large diameter insulating channels, and

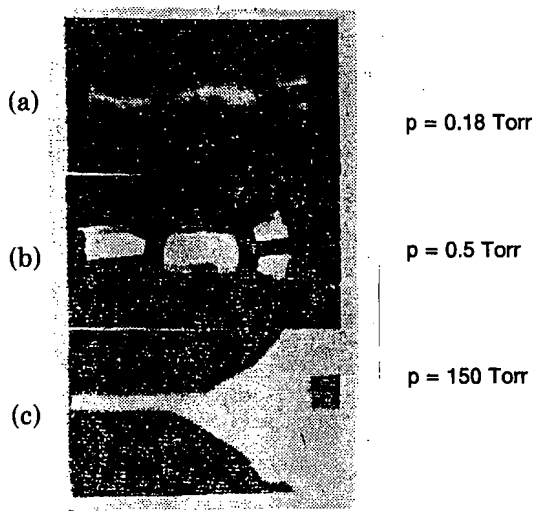


Fig. 22—Photographs of background gas glow [13]

through free space by forming two channels for the return current flow—one in the area of the electron beam itself and the other in the thin cylindrical layer around the beam. The latter shorted the beam current to the accelerator while maintaining beam self-focusing. In addition, the plasma layer had a stabilizing effect upon the lateral oscillations of the beam improving IREB transport.

A quickly developing instability was also observed when IREB propagated in background gas at the pressure of about 100 Torr, leading to a collapse of the electron beam (Fig. 22c).

Experimental measurements of the energy spectrum were made for a 1 MeV, 37 kA IREB injected into a 2 m drift tube filled with air at various pressures (Fig. 23) [3,15,16]. Figure 23 shows that the beam electrons with less than the maximum energy are located in two groups, one at the front of the beam pulse and the other at the end of the pulse. The amplitude of the electron current pulse increased with increasing electron energy and peaked at the maximum electron energy [3]. This beam energy structure maintained its form over the 2 m transport distance in the pressure range of 0.6 to 1 Torr. At 20 Torr, the energy spectrum changed considerably after 1 m distance (Fig. 23b). In this case, both the energy peak and the peak at the end of the pulse are decreased considerably. With further increase in background pressure to 50 Torr, both the energy peak and the peak at the end of the pulse have disappeared completely (see Fig. 23c). Further measurements demonstrated the shortening of the current pulse length at pressures greater than 20 Torr (Fig. 24) [3]. This pulse shortening was attributed to current cutoff allowing only the front of the beam pulse to pass through the dense gas.

It was also determined that at long beam transport distances the pulse current cutoff appears at lower pressures in the drift tube. This current cutoff is attributed to beam instability in dense plasma, which, in turn, is created by the ionization of the neutral background gas. The IYaF-TPI researchers mentioned in 1975 [3] that experiments were being carried out at that time to clarify the mechanism and the specific instability characteristics that are responsible for the above current cutoff.

The 1977 experiments [15] also showed the existence of an optimum pressure of about 1 Torr when the IREB energy spectrum was least perturbed during transport. The maximum energy $E_m$ and its width at half maximum $\Delta E/E_m$ were found to be $E_m \approx 1$ MeV and $\Delta E/E_m \approx 20$ percent. Typical oscillograms of the electron beam current pulse as obtained at the end of 0.8 and 2 m drift tubes at various pressures are shown in Fig. 25.

Beam transport was found to be most efficient when the beam self-fields were fully neutralized along the whole length of the beam path.

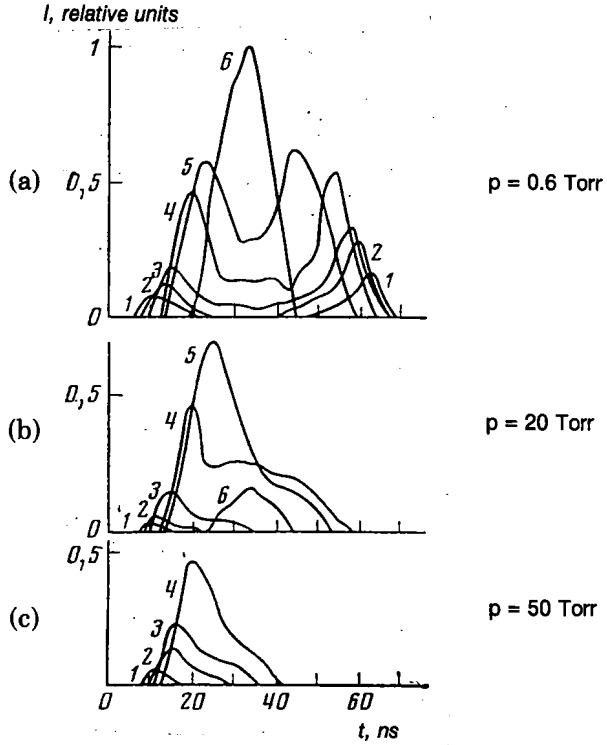


Fig. 23—Energy spectrum time scan of a 1 MeV maximum energy IREB with a 37 kA current pulse at a 1 m transport distance at different background pressures [3]

This occurred at 1 Torr, with the form of the IREB pulse practically unchanged (Fig. 25a and b, curve #3). The behavior of $E_m$ as a function of pressure and transport length is shown in Fig. 26.

Away from 1 Torr, $E_m$ was observed to be displaced toward smaller energies while the beam energy spread increased. This behavior of $E_m$ is not attributed to energy loss from gas ionization.

Below $p_{opt}$, the leading edge electrons were scattered by space-charge forces. The nose erosion placed the $E_m$ electrons at the leading edge of the pulse, and not at the location of maximum current as in the case of $p_{opt} \approx 1$ Torr. The current peak was displaced toward energies

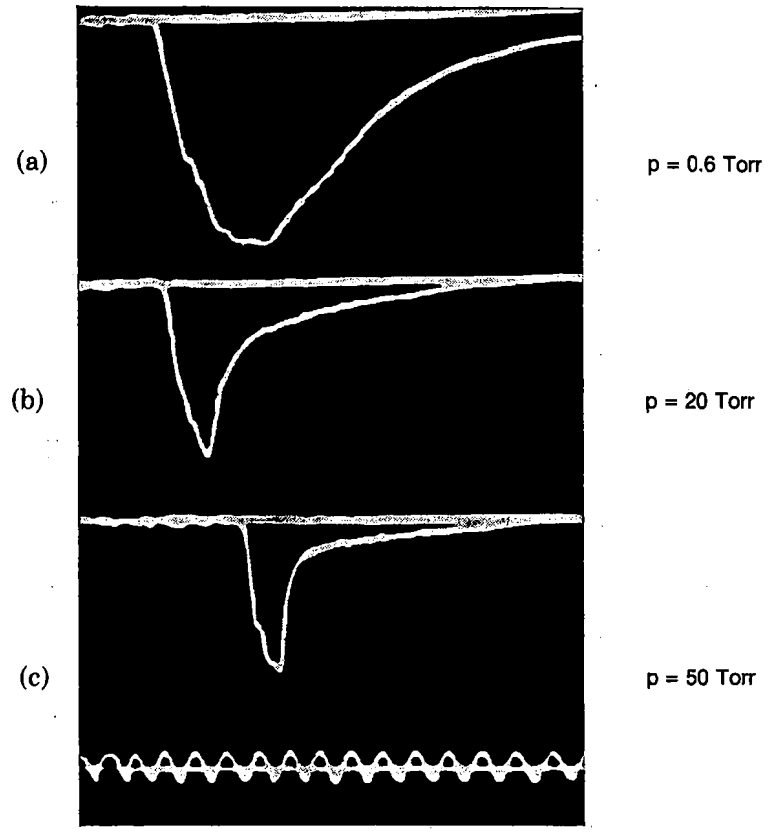


Fig. 24—Beam current pulse oscillograph trace for IREB transport in air at a distance of 1 meter [3] (reference oscillation frequency = 100 MHz)

lower than $E_m$, thus forming the trailing edge of the pulse during the acceleration process. This was the reason for the absence of the high electron energy component in the beam spectra and the $E_m$ shift toward lower energies. Above $p_{opt}$, the front part of the beam propagated more efficiently. Above 5 Torr (Fig. 25b), beam transport terminated before the $E_m$ electrons could appear. These factors lead to the same spectra change as in the case for pressures lower than $p_{opt}$.

The Soviet researchers concluded that the observed variation in beam energy spectra in beams transported in neutral gas at various pressures is due to the different propagation effectiveness of the various parts of the beam. This effect is maintained by the transient

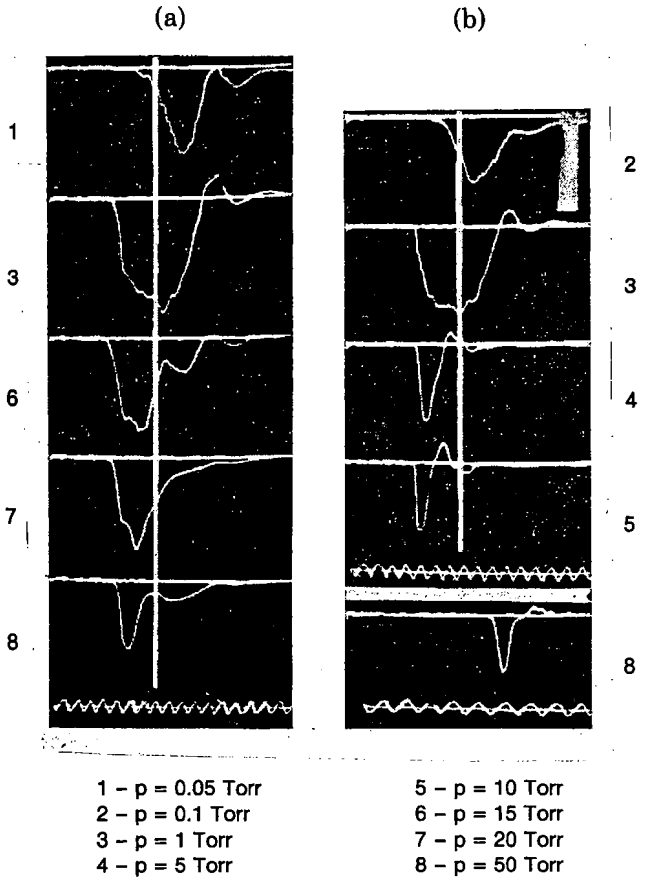


Fig. 25—IREB current pulses at the end of the drift tube (a) 0.8 m and (b) 2 m at various background gas pressures [15]. The vertical line denotes the location of electrons with energy $E_m$

IREB energy structure determined by the acceleration process. To maintain an unchanged energy character of the beam under transport it is necessary to insure conditions that allow full neutralization of the beam's self-fields along the whole path of transport [15].

Control of the length of the IREB current pulse was investigated in 1977 using the principle of beam current cutoff during its transport in neutral gas at pressures higher than $p_{opt}$ [17]. These tests were also carried out with the Tonus accelerator at 1 MeV, 40 kA, and a drift tube 2 meters long. The current pulse length was controlled by varying the pressure within the drift tube. The dependence of the pulse length

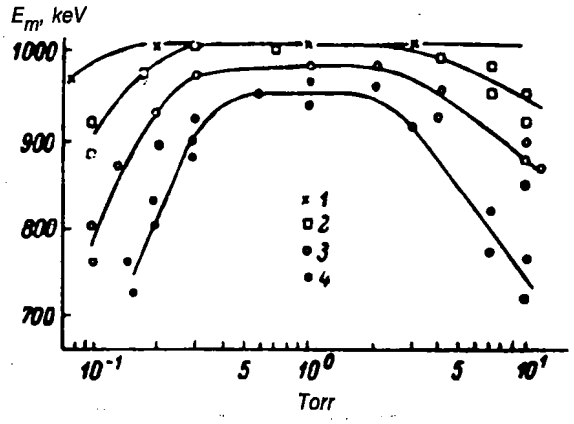


Fig. 26—Value of the energy at the maximum current peak $E_m$ as a function of pressure p and transport length L [15]

on background pressure and transport length is shown in Fig. 27. Pulses shorter than 10 ns can easily be obtained by this method.

Other experiments at IYaF-TPI made in 1977 on plasma channels induced by an IREB propagating through gas and air indicated that the beam tracked the plasma channel configuration. These experiments were made with the Tonus accelerator with a 1 MeV, 35 kA, 60 ns beam injected into a drift space filled with air [14]. The most effective IREB transport was achieved at a background air pressure of 0.09 to 0.6 Torr. At the pressure range of 0.14 to 0.17 Torr long wavelength "hose" instabilities were observed with a large lateral displacement of the beam. At pressures higher than 0.6 Torr, the beam defocused because of an increase in beam current neutralization [14].

The above research included Usov's well-known experiment with a 1 MeV beam in a large gas-filled drift chamber. In a homogeneous transverse magnetic field, the radius of curvature of the beam trajectory was determined by the 0.5 MeV nose of the pulse, and not by its 1 MeV peak energy, thus indicating that the beam could track the plasma channel.

The researchers at IYaF-TPI stress the importance of the effect of collective fields generated by the beam itself and the beam's interaction with the plasma channel. These researchers also found that an IREB can be effectively transported across a magnetic field along localized

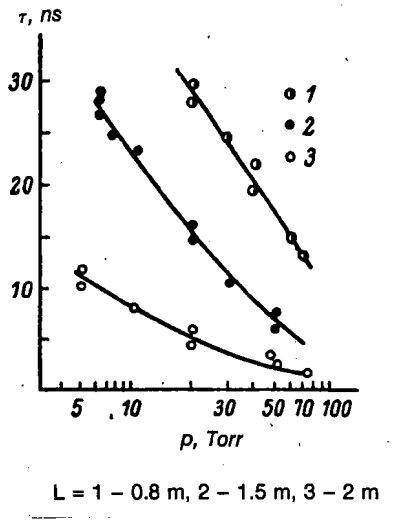


Fig. 27—Pulse length as a function of background pressure and transport length, L [17]

plasma channels having diameters smaller than that of the electron beam as well as along thin conducting wires. The effectiveness of transport was found to be determined by the degree of magnetic and electrostatic neutralization of the beam [14].

# III. IAE RESEARCH ON HOSE INSTABILITY

Researchers at the Kurchatov Atomic Energy Institute (IAE), under the leadership of L. I. Rudakov, carried out experiments from 1974 to 1978 using the MS accelerator at 0.4 MeV, 40 kA, 40 ns to investigate beam transport and the formation of plasma channels with the help of external magnetic fields for beam focusing. The experiments demonstrated poor beam transport at background air pressures higher than 0.5 Torr [18,19].

Since 1982, IAE researchers have studied the resistive hose instability of an IREB beam injected into air and gases [20,21]. Resistive hose instability is the result of resonant interaction of magnetic field oscillations with betatron oscillations of beam particles and is observed as macroscopic transverse beam oscillations, which eventually deflect the beam completely off axis and onto the wall of the drift tube.

The formation time of hose instability was found to be considerably shorter than the characteristic time of plasma magnetic field decay. The distance at which the instability begins to oscillate is of the order of several betatron oscillation wave lengths. The time and length of the instability formation decreased with increasing pressure from 1 to 100 Torr.

Experiments with resistive hose instability were carried out using the "Neptun" accelerator at 450 keV, 20 kA, and pulse length of 60 ns. The beam electrons passed through a 20 micrometer thick titanium foil and were injected into a drift chamber filled with $N_2$, $H_2$, or air at various pressures. The beam transport distance was varied from 3 cm to 3 m and the pressure within the chamber was varied from 1 to 100 Torr [20,21].

The measurements involved radial distribution of total beam current density at different distances from the point of beam injection at different pressures. Typical scans are shown in Fig. 28 [20]. At 1 Torr, the current density distribution maintained its axial symmetry to a distance of 0.8 m (Fig. 28a). As beam transport distance increased, this symmetry was perturbed (Fig. 28b) first at the trailing edge of the pulse. In some cases, beam deflection was less than the beam radius at a distance of 2 meters, but at 3 meters at the pulse trailing edge, the beam was deflected by more than the beam radius. As gas pressure increased, the asymmetry of the beam current density profile and beam deflection also increased (Fig. 28c).

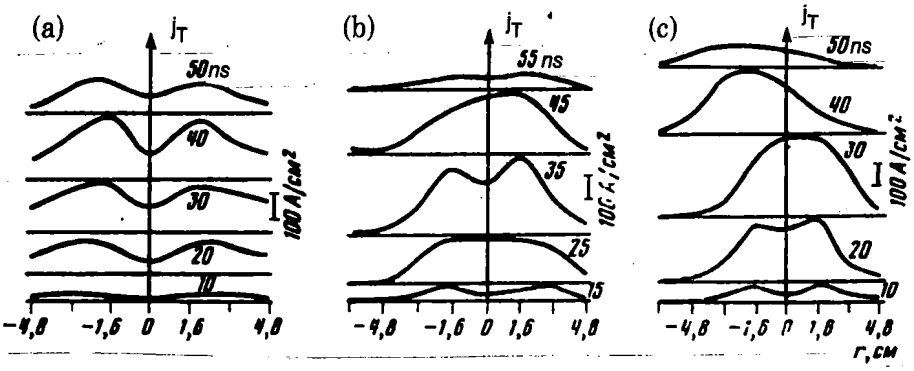


a – p = 1 Torr, L = 26 cm
b – p = 1 Torr, L = 85 cm
c – p = 5 Torr, L = 85 cm

Fig. 28—Beam current density radial distribution at different times after injection [20]

The measurements [17,18] showed that the distance at which the beam is thrown from the axis into the chamber wall depends upon pressure (Fig. 29) and decreases with increasing pressures.

The data obtained from Faraday cups were in good agreement with optical observations of plasma scintillation in the drift chamber obtained from electron-optical converter photographs (Fig. 30).

Figure 30a shows three consecutive photographs of the beam thrown off axis onto the chamber wall at 30 Torr. In 10 to 15 ns, the beam remained close to the axis of the chamber; in 15 to 20 ns, the beam moved radially through about one radius; and in 20 to 25 ns, the beam was thrown completely onto the chamber wall. At 60 Torr (Fig. 30b) the beam is thrown to the chamber wall in only 11 ns. The characteristic excitation length was 45 cm at 30 Torr and 30 cm at 60 Torr. The average transverse displacement velocity was found to increase with pressure, changing from $5 \times 10^8$ to $2 \times 10^9$ cm/s, for a pressure change 5 to 60 Torr, respectively [20].

The experiments demonstrated that the beam trajectory instability develops in a spiral that unwinds toward the end of the drift tube and that beam asymmetry is accompanied by beam rotation around its axis. The angular velocity of this rotation was $3 \times 10^8$ sec$^{-1}$ and was observed in both left and right directions. The instability was found to possess a weakly convective character with an oscillation drift velocity less than $10^2$ cm/s. At pressures greater than 10 Torr, the transverse oscillation amplitudes were found to be so high that a large part of the beam was thrown to the chamber wall.

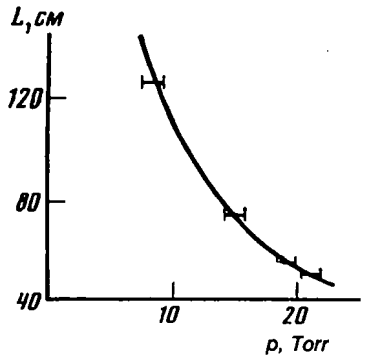


Fig. 29—Distance to off-axis displacement as a function of pressure [20]

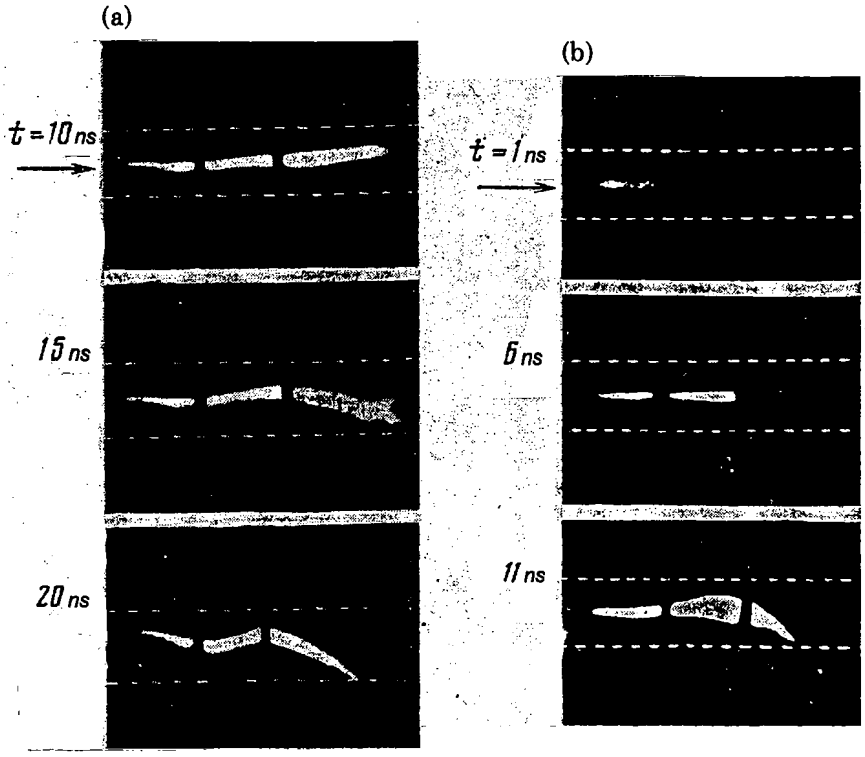


a – p = 30 Torr, L = 1.3 m
b – p = 60 Torr, L = 1.3 m

The arrow represents the direction of the beam injection. The horizontal dotted lines represent the position of the chamber wall. The vertical dark lines are axial distance markers located 20 cm apart

Fig. 30—Electron-optical converter graphs of axial displacement [20]

IAE researchers state that the accuracy of their time measurement in the observations of plasma scintillation due to the propagation of the beam was within 1 ns. The plasma channel formed by the beam was observed to remain for more than 100 ns after the passage of the electron beam pulse [20].

The current density distribution in the cross sectional plane of the transport chamber was measured as a function of time (Fig. 31) [20]. The figure shows the asymmetry, displacement, and rotation of the beam in the cross sectional view. Oscillograms of signals from a beam collector placed at the location where the beam was thrown from the axis (at L = 85 cm) at p = 15 Torr are shown in Fig. 32 [20].

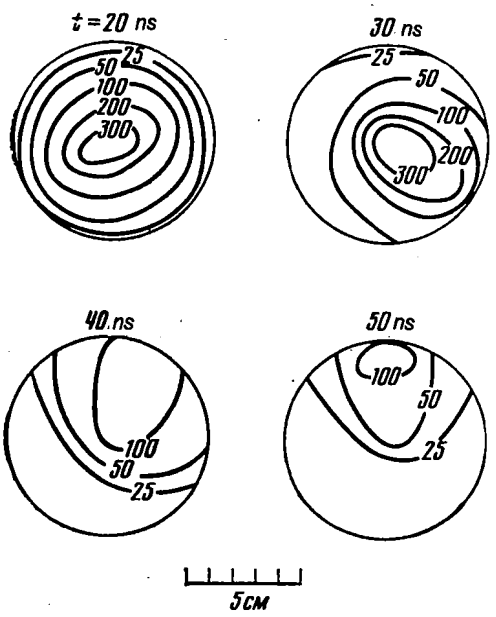


Fig. 31—Beam current density distribution (in A/cm$^2$) as a function of time [20]

The beam propagated symmetrically during the first 15 ns; for the next 10 ns the beam disappeared from the collector's field of view and reappeared on one side of the collector's face. The beam was displaced radially with a velocity of $10^9$ cm/s.

The time of plasma magnetic field decay in these pressure ranges was longer than 100 ns for a 3 cm beam radius and plasma conduc-

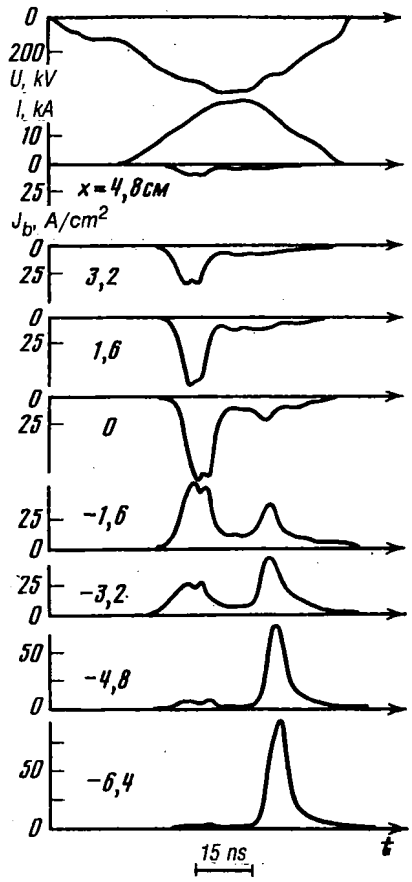


Fig. 32—Oscillograms of the voltage V, diode current I, and beam current density $J_b$ as measured with sectioned Faraday cups located at different distances from the chamber axis [20]

tivity $\sigma \geq 10^{12}s^{-1}$.[1] The beam instability developed in considerably less time (t = 1 to 20 ns) than the magnetic field decay time.

Recent theoretical work at IAE on the resistive hose instability led to the conclusion that under conditions of above experiments [20,21],

[1]In the investigation of the plasma magnetic field decay time, Soviet researchers do not differentiate between the monopole time constant $\tau_m$ and the dipole time constant $\tau_d$. The time constant to which the Soviets refer with a value of 100 ns is probably $\tau_m$, which is observed for the plasma current at the tail of a beam current pulse. The value of the dipole decay time constant $\tau_d$ would be 5 or 10 times shorter. The hose instability builds up on the time scale of $\tau_d$.

an external axial magnetic field of 6 kG applied to the IREB can totally dampen short-wave oscillations causing hose instability. The long-wave oscillations do not have time to develop for the meter propagation length conditions in these experiments [22].

Theoretical analysis was also applied to beam self-focusing produced by two effects in plasma: (1) increase of beam space charge neutralization with increasing plasma density and (2) generation of magnetic field by thermo-convective currents in inhomogeneous plasma. IAE researchers made a calculation to demonstrate the degree of compression of a beam with parameters of 5 MeV, 60 kA, r = 3 cm, in a plasma with a density of $10^{16}$ $cm^{-3}$ that extends along the beam direction for a distance of $L \simeq 50$ cm. The generation of the magnetic field during plasma heating in the beam relaxation process was found to lead to beam compression with a compression factor of 10 [23].

Other recent theoretical work at IAE included the research on the resonant helical instability of an IREB [24] and the study of the generation of a magnetic field in combination with the filamentation of an IREB propagating through a plasma with strong current neutralization [25]. These studies showed that for typical experimental parameters for IREB passing through gases and plasma (for beam currents from 30 to 100 kA, $r_b$ = 1 to 2 cm, and the plasma density of about $10^{14}$) helical instability is present and fast oscillations are excited causing local compression of the beam [25].

The expulsion of magnetic field from the electron beam by hot electron gas whose pressure is greater than the pressure of the magnetic field has also been recently investigated [26]. In this theoretical analysis, the expulsion process in a high-conductivity medium was shown to be accompanied by a rearrangement of the magnetic field in a time considerably shorter than skin effect time $\tau_{sk}$ ($\tau_{sk} = 4\pi\sigma r^2/c^2$, where $\sigma$ = conductivity, $r$ = characteristic size of the current flow area) [26]. Nonlinear wave solutions have been obtained for a constant dispersion velocity, which can be considerably lower than the velocity of fast electrons.

# IV. FIAN-IOF RESEARCH—EXPERIMENTAL BEAM PROPAGATION STUDIES

During the early 1970s, experimental work at the Lebedev Physics Institute (FIAN) involved general properties during beam transport through gases. Since 1981 FIAN, together with the newly formed Institute of General Physics (IOF) under the leadership of A. A. Rukhadze, has been publishing experimental studies of beam current enhancement, thermal effects within the IREB, and their effect on the background gas density.

The first experimental results concerning the perturbation of air density by an IREB pulse were published by FIAN-IOF in 1984 [27]. The gas dispersion after the initiation of the beam pulse was analyzed numerically [28]. In the latest experiment beam parameters were measured and gas density change was determined along the beam axis [29]. A simple relationship was found between the measured gas density distribution after the beam pulse and the input energy profile [29].

The behavior of gas density after the injection of an IREB pulse was observed [27] experimentally using the Terek-1R accelerator [30,31] with beam currents of 10 to 15 kA, beam energies of 1.5 MeV, and pulse lengths of about 60 ns. The current densities on axis were 0.3 kA/cm$^2$ and 1 kA/cm$^2$ with the beam radius of 1.5 to 3 cm. The beam was injected into atmospheric air through a 50 $\mu$m thick titanium foil.

The gas density radial distribution for different times after beam injection is represented in Fig. 33 [27]. There were considerable differences in the behavior of background gas with different beam current density values. This type of gas behavior could be explained simply by the difference in energy input; FIAN-IOF researchers attribute it to the energy accumulated in the internal degrees of freedom of the gas and to the strong dependence of relaxation time on gas temperature. The relaxation time was said to be determined by the input energy of the beam. This gas behavior can also be seen in the dependence on time of the rarified gas density along the beam axis after beam injection as shown in Fig. 34 [27].

The dependence of the maximum amplitude of the gas compression coordinate upon the time after the beam injection with a current density along the beam axis of $j$ = 1 kA/cm$^2$ is represented in Fig. 35 [27].

These experiments determined that the velocity of the compression wave outside the volume occupied by the beam itself ($r \geq 3$ cm) is close

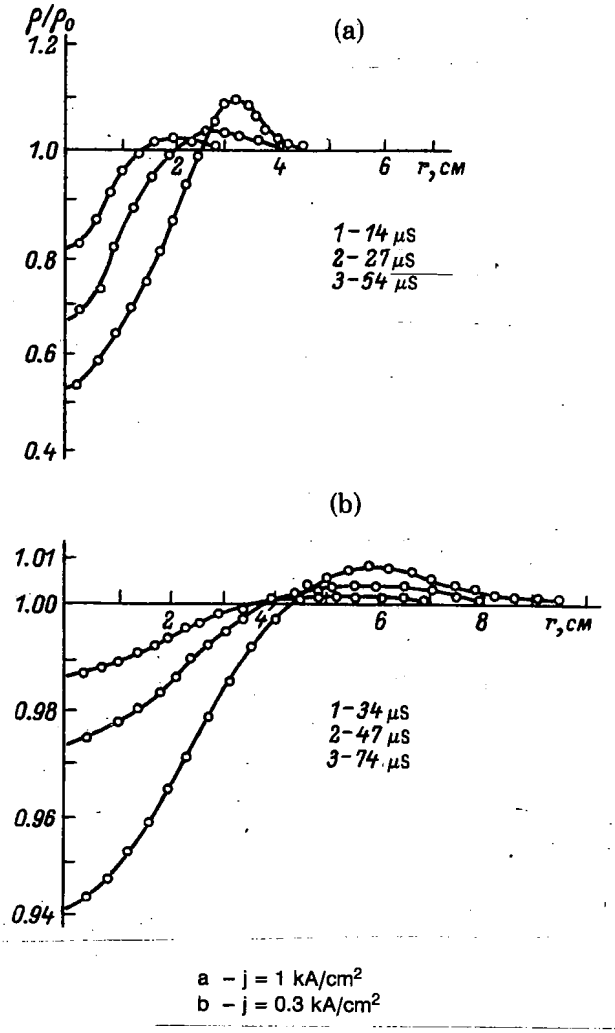


Fig. 33—Gas density radial distribution at different times after beam injection [27]

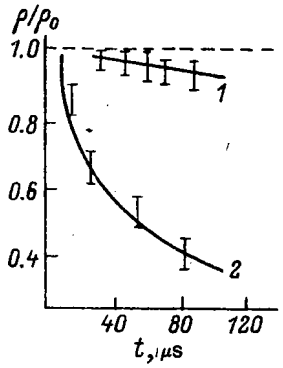


1 – j = 0.3 kA/cm$^2$
2 – j = 1 kA/cm$^2$

Fig. 34—Gas density along the axis of the beam as a function of time after the IREB injection [27]

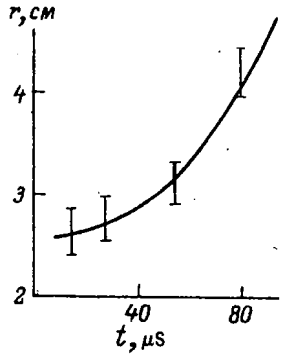


Fig. 35—Maximum amplitude of the gas compression coordinate as a function of time after the beam injection for j = 1 kA/cm$^2$ [27]

to the velocity of sound. The investigation of the density behavior after IREB injection can be a valuable source of information about the relaxation kinetics of the oscillation-induced conditions.

The decrease in gas density along the beam trajectory was further experimentally investigated [29] using the Terek-1R accelerator with beam currents from 4 to 15 kA at beam energies from 1 to 1.2 MeV and pulse lengths of about 60 ns. A relationship was determined between gas density distribution after the IREB pulse and the energy deposition profile. A typical gas density distribution $\delta\rho(r)$ for $t_{observed} = 34\ \mu s$ is shown in Fig. 36a [29]. The radial distribution of the beam energy release into the gas is shown in Fig. 36b [29].

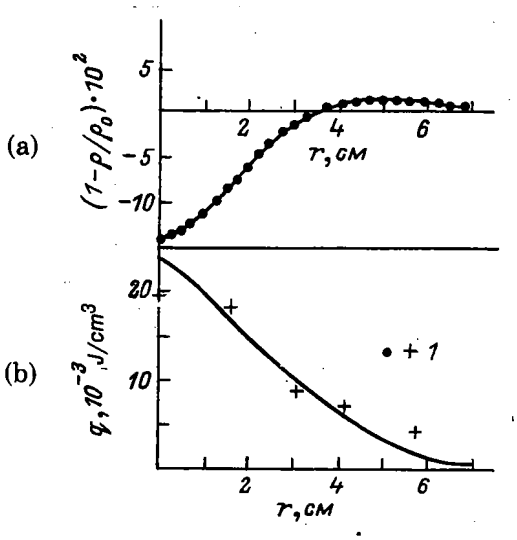


Fig. 36—a – Gas density radial distribution observed 34 $\mu$s after the IREB pulse [29]
b – Radial distribution of the beam energy release into the gas

The gas density change along the beam axis as a function of time is shown in Fig. 37 [29]. The minimum value of gas density near the beam axis can be seen from Fig. 38 where its dependence on $p/p_o$ is in good agreement with theoretical calculations. Another issue was the total beam current enhancement when the plasma electron current flows in the same direction as the IREB and its total amplitude can exceed the amplitude of the injected beam. Researchers at Yefremov

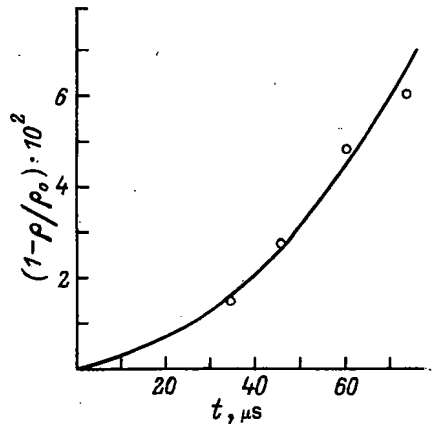


Solid line – theory
o – experimental observations

Fig. 37—Dependence of the gas density along the beam axis upon time [29]

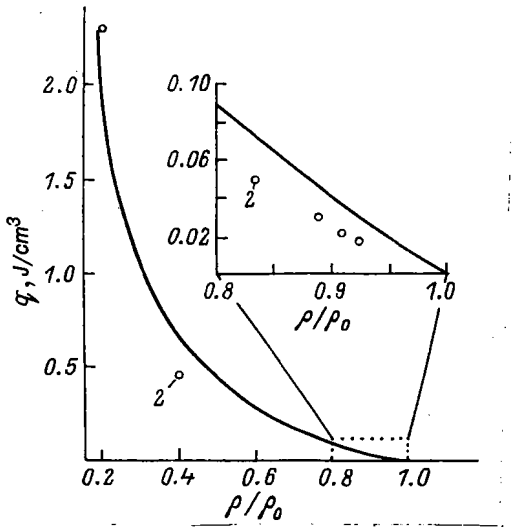


Solid line represents calculated values
Data points represent experimental observations made in Ref. 27

Fig. 38—Dependence of the released energy density along the beam axis upon the change in gas density at $t_{observed} \gg t_s$ [29]
here: $t_s \simeq \frac{\alpha}{C_s}$ where $\alpha$ = effective beam radius
$C_s$ = velocity of sound

(NIIEFA) observed the amplification of the beam current in 1978–1979 [32,33] and they were able to correlate this experimental finding with the movement of plasma electrons in the turbulent fields of a plasma-beam instability.

The current enhancement was experimentally determined [32,33,34,35] to be due to two-stream instability. However, in 1984, FIAN-IOF researchers observed beam current enhancement at pressures close to atmospheric, contrary to what these experiments led them to believe [36].

Again using the Terek-1R, with 7 kA, 1 MeV, and 60 ns pulse length, the beam was injected into air, He, $SF_6$, and a mixture of $SF_6$ + He + $H_2$. The experiments were carried out both with an axial magnetic field ($B \approx 2.4$ kG) and without a magnetic field.

The experiments have shown nanosecond spikes with amplitudes several times higher than that of the injected beam. This effect was observed for all gases at all distances from the point of injection.

The characteristic length of the spike in the total beam current pulse was found to correspond to the time of beam neutralization [30]. This was assumed to be the effect of current enhancement at the beam front. The spike structure of the pulse was visible with pressure starting from several tens of Torr at distances greater than 1 meter with the spike amplitude increasing toward the end of the pulse [36]. The application of the axial magnetic field completely obliterated this effect even at pressures close to atmospheric. The effect was most prominent in helium, but it was also observed in the other gases.

The effect of total beam current enhancement was attributed to the appearance of the spikes in the current pulse. At fairly high pressures and at transport distances of greater than 1 meter, at the end of the total current pulse a nanosecond peak was observed that was a factor of 1.5 greater than the amplitude of the injected beam current. This effect of beam current enhancement increased with transport distance and with increase in background gas pressure (Fig. 39) [36].

In He, even at $p = 750$ Torr, the peaks could not be dampened with the axial magnetic field, although other gases did not show this effect. There was thus a difference in the conductance of the beam plasma in He than in the other gases. FIAN-IOF researchers are at present investigating this beam current enhancement theoretically [36].

Other experiments performed with Terek-1R included plasma return current induced by IREB and concentration and temperature of beam-produced plasma, using laser dispersion [37]. At pressures greater than 3 Torr, plasma concentration increased to $5 \times 10^{16}$ cm$^{-3}$ at a temperature of $T \sim 1$ eV, which demonstrates the presence of collective processes that take place in the plasma. For these experiments the

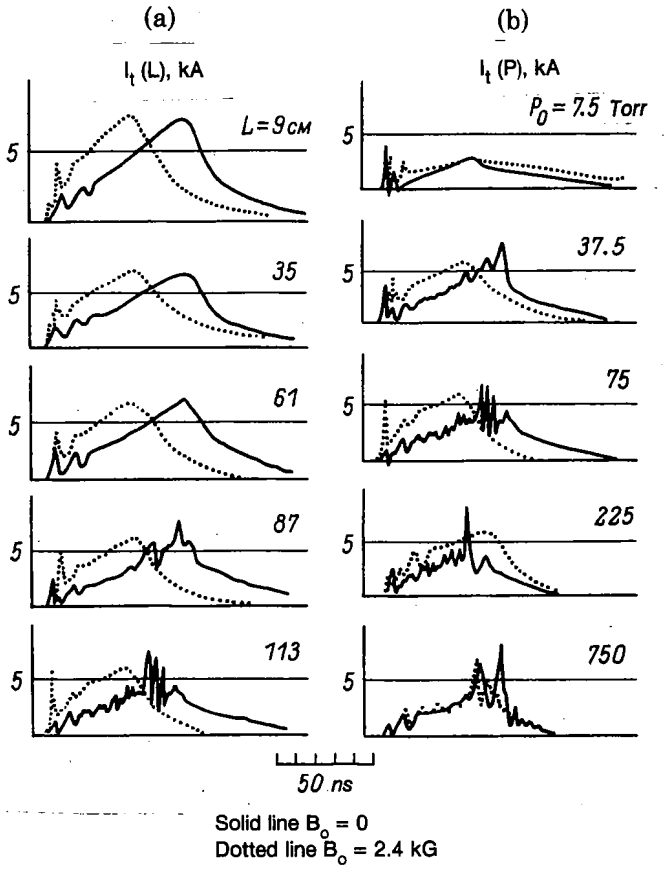


Fig. 39—a – Total beam current as a function of distance from injection at a pressure of 75 Torr in He [36]
b – Total beam current as a function of pressure in He at a distance of 113 cm from injection

accelerator was operated with a beam current of 25 kA at 1.5 MeV with a 60 ns pulse length.

The Terek-1R was used in 1984 in a set of experiments on the investigation of beam pulse front erosion by neutral gases at pressures from 100 to 750 Torr [38]. These experiments were performed at 1.5 MeV, 12 kA, 40 ns using a drift tube 1.2 m long. The gases used were nitrogen and a mixture of $N_2$ and $SF_6$ (in the ratio of 6 to 1.) The beam transport through the drift tube was carried out with and without the application of an axial magnetic field of about 5.8 kG. Erosion of the leading front of the beam pulse was observed to increase with beam

transport length. At a distance of 60 cm, the pulse width was shortened to half its original width. With the application of the axial magnetic field this effect of pulse front erosion completely disappeared. The erosion of the pulse front was observed over the whole pressure range from 100 to 750 Torr, and any quantitative effect of the erosion was found not to depend upon gas pressure [38].

Another set of experiments was performed in 1984 on the injection of IREBs into gas at these high pressures but with lower beam current densities ($j_b \leq 50\ A/cm^2$). The Terek-2 accelerator was used for these investigations with beam energy of 360 keV and beam currents of 1.4 kA and 250 A [39].

In experiments performed earlier at FIAN using the Terek-1R [30], a dependence of the plasma return current upon the beam current as a function of background gas pressures was obtained. In subsequent experiments [37] the reverse current was found to have a maximum in the neighborhood of $p \sim 1$ Torr just where a considerable concentration of plasma electrons was found (Fig. 40) [37]. As pressure increased, the role of cumulative ionization (ionization by secondary electrons) decreased and direct gas ionization by the IREB became responsible for the formation of the plasma.

The FIAN-IOF researchers stressed the significance of their research to optimal IREB transport through gas, as well as to high-power gas lasers and plasmo-chemical reactors. The results were also claimed applicable to IREB diagnostics in gas, where the measurements of the electron beam parameters give no single-valued results or perturb the distribution of induced currents or fields.

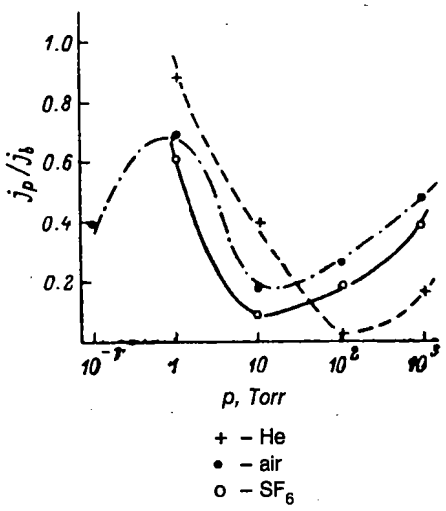


Fig. 40—Plasma current to beam current ratio as a function of gas pressure [37]

# V. KhFTI EXPERIMENTAL RESEARCH ON BEAM PROPAGATION

KhFTI's experimental research on the propagation of IREBs through background gas or plasma can be broken down into two separate groups. One group, whose publications extend from 1973 to 1982 under the leadership of Yu. V. Tkach and Ya. B. Faynberg, has investigated IREB propagation through air using a 1 MeV, 50 kA, 30 ns electron beam with transport distances of up to 3 m. The second group, headed by Ya. B. Faynberg with A. K. Berezin as a leading author, and publishing from the early 1970s to 1981, used a 2 MeV and a 20 MeV linear electron accelerator with low beam currents of 0.5 to 1.0 A and investigated the interaction of IREB with air and plasma. No papers of KhFTI researchers have been found since 1982.

The early work of the first group, dating back to 1973, dealt with the formation of return current, the optimum pressure for transport in air, and the measurement of the ionization front velocity in various gases in the pressure range from $5 \times 10^{-2}$ to 10 Torr [40]. In 1980, the effect of collisions upon the beam relaxation and of collective and elementary processes upon energy transport through gas were studied [41]. The later experiments used a 0.7 MeV, 30 to 35 kA electron beam, 40 ns pulse length, with transport distances up to 3 m in air, in the pressure range from 0.1 to 100 Torr, without the presence of external magnetic fields.

The KhFTI researchers claim to have demonstrated experimentally that the relaxation of an IREB in a neutral gas and plasma without external magnetic fields occurs mainly through collective processes, which, during their formation, are accompanied by the excitation of an intensive microwave and X-ray radiation from the plasma, the modulation of the IREB, and the formation of a fast group of particles with energies reaching 20 to 30 keV. According to computer simulation, in addition to the collective processes, an important role is played by elastic scattering of the beam particles on the plasma atoms and ions, which removes particles from the beam channel if the scattering angle is greater than a certain critical value.

The KhFTI researchers devised complex diagnostics for these experiments to obtain accurate measurements. A series of Rogowski loops monitored the diode and beam currents at various locations along the drift tube, a 25-strip calorimeter measured the total beam energy and its radial distribution and allowed control of the beam diameter while

making calorimetric measurements, a 12-channel magnetic analyzer determined the spectral distribution of the beam electrons, and a 4-channel X-ray spectrometer measured bremsstrahlung radiation emanating from the plasma heated by the IREB.

The KhFTI researchers stressed the importance of transporting energy to large distances and mentioned that the most important characteristic is the beam energy density obtained on target as a function of background gas. The measured energy carried by the beam over different distances as a function of pressure is shown in Fig. 41. The energy carried by the beam as a function of distance for various pressures is shown in Fig. 42. The condition for maximum energy carried by the beam to a certain distance is shown in Fig. 43 as a function of pressure [41].

From their experimental measurements, the Soviet researchers concluded that in order to obtain the maximum energy carried by the beam for short distances ( $\leq$ 50 cm) it is necessary to choose the pressure at which the beam is self-focusing at $p \simeq 1$ Torr. To carry the beam over long distances, it is necessary to take beam energy dissipation into account. The optimum gas pressures for long distance beam transport were found between 0.2 and 0.6 Torr [41].

The changes in particle velocity and particle density in beam propagation through gas were measured experimentally. The beam energy spread was measured at the output of the accelerator and at various locations along the drift tube as a function of gas pressure and was

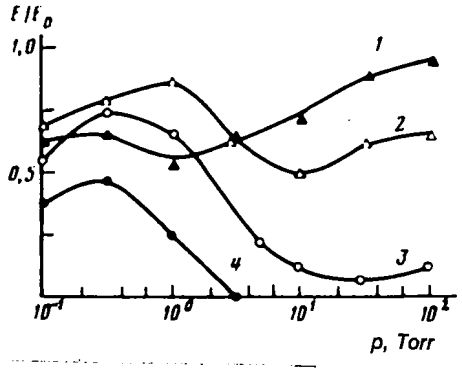


$I_b$ = 30 kA, $r_b$ = 1.8 cm, $R_c$ = 5.5 cm; z is path length:
1 – z = 6 cm
2 – z = .5 m
3 – z = 1 m
4 – z = 3 m
$E_0$ = maximum measured beam energy

Fig. 41—Energy carried by the beam to different distances as a function of gas pressure [41]

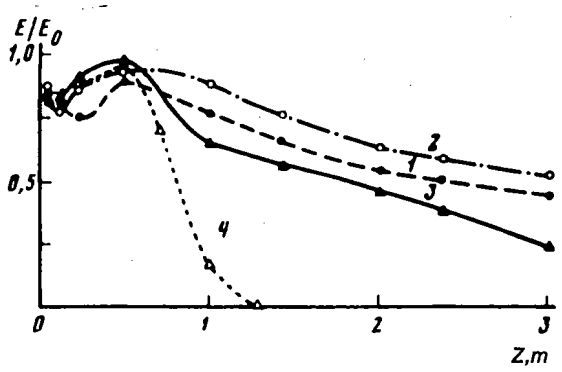


$I_b$ = 30 kA, $r_b$ = 1.8 cm, $R_c$ = 5.5 cm
1 – p = 0.1 Torr
2 – p = 0.4 Torr
3 – p = 1 Torr
4 – p = 10 Torr

Fig. 42—Energy carried by the beam as a function of distance for various gas pressures [41]

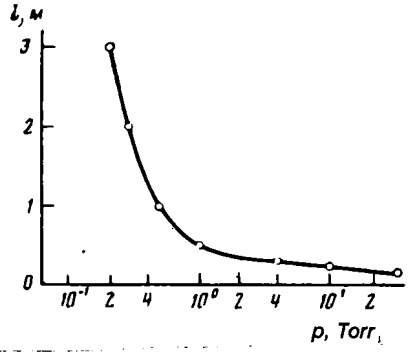


$I_b$ = 30 kA, $r_{collector}$ = 3 cm, $r_b$ = 1.8 cm,
$R_c$ = 5.5 cm

Fig. 43—Pressure required for maximum energy carried by the beam to different distances [41]

represented as a time function for two pressures in Fig. 44 [41]. At the optimum transport pressure of $p$ = 0.4 Torr, beam energy distribution changed only slightly with change in transport distance (see Fig. 44). At high pressures, the beam energy peak was shifted to the lower energies and the low energy particles decreased with increased z, while the pulse shortened.

The beam energy spread was determined as a function of gas pressure for several transport distances (Fig. 45) [41]. The energy spread was independent of p and z at short transport distances, but it was markedly dependent at the 3 m point.

Further analysis of their data allowed the researchers to calculate the specific beam particle energy as shown in Fig. 46 demonstrating a much larger beam energy loss in the pressure region of 0.1 and 1 Torr than in the region of 0.3 to 0.6 Torr.

The researchers noted that at the pressure range of 0.1 to 0.2 Torr, the increase in energy loss was due to incomplete space charge neutralization and deceleration of the beam by the space charge field. The increased loss in the 1 to 3 Torr range was due to collective processes accompanied by microwave radiation. The dependence of microwave

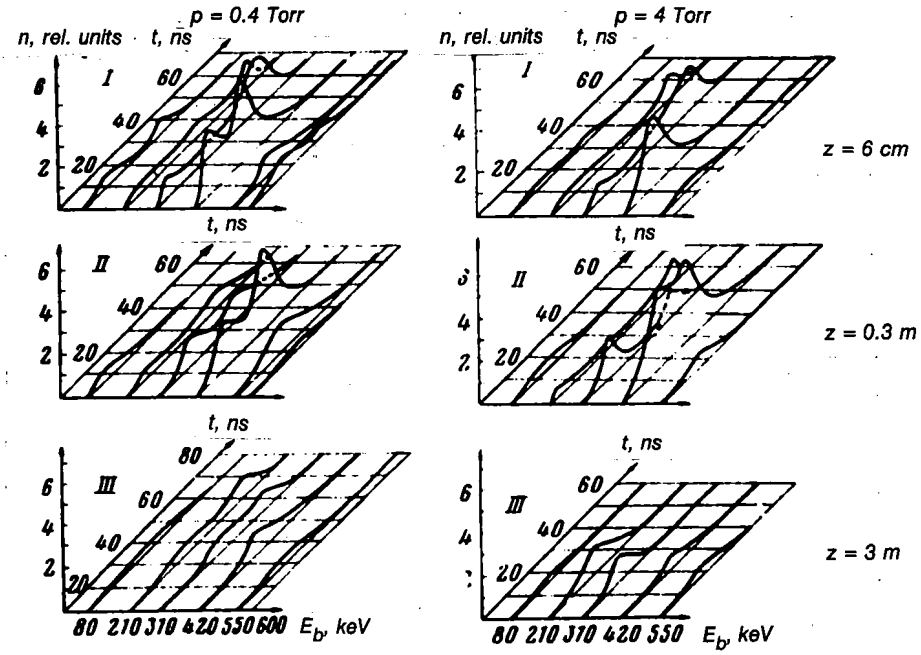


Fig. 44—Time plots showing the IREB energy spread at three locations along the drift tube for p = 0.4 and 4 Torr [41]

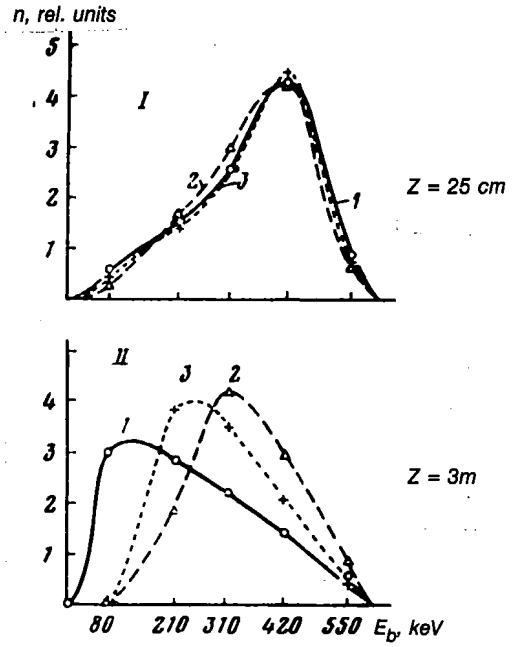


Fig. 45—Beam energy spectra as a function of background pressure at two transport distances [41]

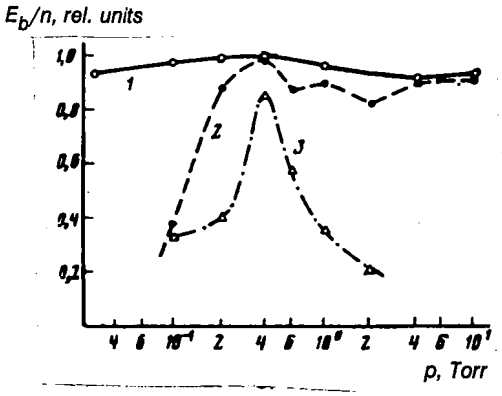


Fig. 46—Specific energy of the transported electron beam at different transport distances as a function of gas pressure [41]

radiation intensity upon pressure and transport length is shown in Fig. 47 for the wavelengths of 3 cm, 8 mm, and 1.8 mm.

Figure 47 shows that a microwave radiation peak appears at points in the pressure range where the beam sustains a considerable particle energy loss. The microwave radiation shows a minimum at the point of optimum beam transport. As the beam path lengthens, the range of pressures for which microwave radiation is observed increases.

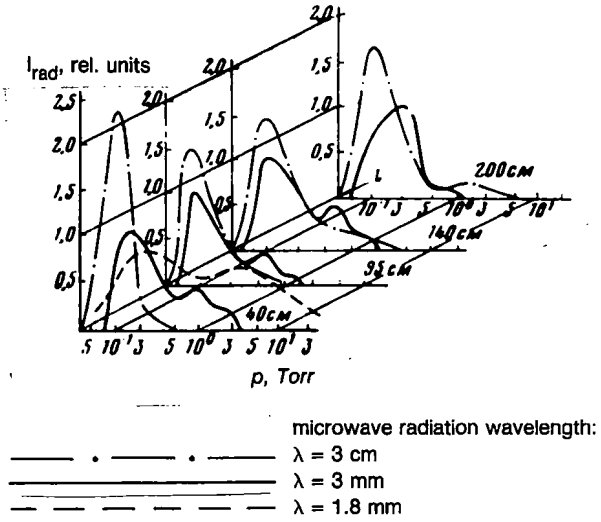


Fig. 47—Dependence of the microwave radiation intensity upon gas pressure and transport length [41]

X-ray radiation emanating from the plasma was found to be fairly weak in the pressure range corresponding to optimum beam transport and to increase at pressures from 0.6 to 3 Torr in the region where the maximum modulation of the beam current was observed. The dependence of the X-ray radiation intensity as a function of gas pressure is shown in Fig. 48 [41].

The angular and radial beam current distribution as a function of gas pressure and time were investigated [42] using a beam current of 30 kA, a beam energy of 0.5 MeV, pulse length of 45 ns, beam radius of 1.8 cm, and background gas pressure from $5 \times 10^{-2}$ to 50 Torr. The findings are shown in Fig. 49. The initially cylindrical radial electron distribution assumed a hollow-beam character at a distance of 40 cm from the point of beam injection. At low pressures (less than 2 Torr) this happens in a time equivalent to the pulse length; at higher pres-

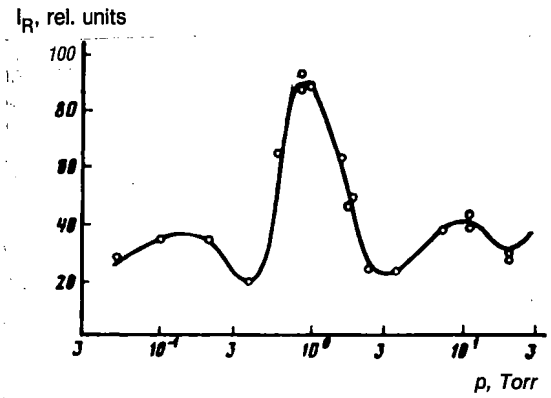


Fig. 48—Dependence of the soft X-ray radiation (15 to 35 keV) emanating from the plasma upon background gas [41]

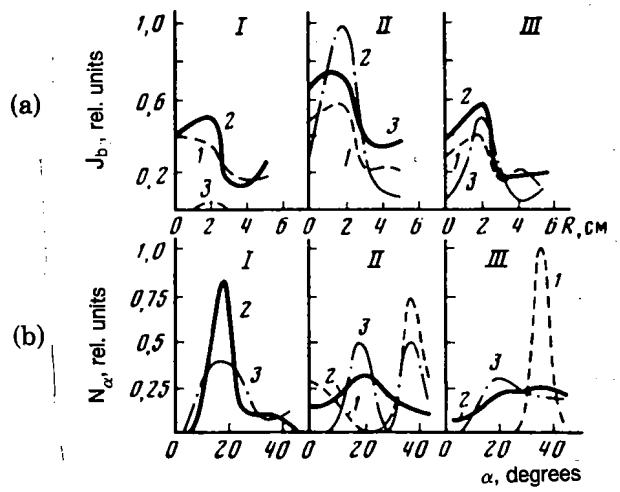


Fig. 49—Radial distribution of beam current density (a) and IREB particle angle distribution (b) in the drift tube for various times and pressures [42]

sures, the beam possesses a well-defined hollow beam structure during the entire pulse.

Using the 2 MeV and the 20 MeV linear accelerators with a current range of 0.5 to 1.0 A, the second group of KhFTI researchers studied the interaction of an IREB with plasma. The early experimental research of this group (1971–1972) concentrated on IREB interaction with low density hydrogen plasma of $10^{10}$ to $10^{13}$ $cm^{-3}$ using the 2 MeV electron linear accelerator at low beam currents of about 1 A [43,44,45]. Later experiments (1974 to 1976) involved high density plasma of $10^{15}$ to $10^{17}$ $cm^{-3}$ [46,47,48]. In experiments carried out in 1979 with the 2 MeV IREB in air at atmospheric pressure, KhFTI researchers demonstrated the formation of a intermediately dense plasma (up to $10^{13}$ $cm^{-3}$) and also observed an effective collective interaction of the electron beam with plasma [49]. The latter was apparent from the considerable loss of beam energy as well as from microwave and soft X-ray radiation localized in the area of beam interaction.

In 1978–1979 the group published two papers on the LU-40 linear accelerator with 20 MeV, 0.5 A, and pulse length of 10 ns [50,51]. Only about 1 percent of the beam passed through plasma with a density of 6 to 8 $\times$ $10^{16}$ $cm^{-3}$. At 2 to 3 $\times$ $10^{16}$ $cm^{-3}$, about 20 percent of the beam could be propagated. However, at a density of 5 $\times$ $10^{15}$ $cm^{-3}$ only about 15 to 20 percent of the beam would be lost.

The energy of the X-ray radiation emanating from plasma varied from 40 to 90 keV, depending on plasma density, with an intensity of $10^5$ $R/cm^2-s$ at 10 cm from the system axis. The Soviet researchers claim that the X-ray radiation measurements correlated well with the observed beam current losses.

The interaction zone between the plasma and beam was less than 10 cm; the beam electrons accelerated by an additional 4 MeV (for an initial beam of 20 MeV). The researchers therefore proposed that high-frequency fields of at least 400 kV/cm have been set up in the interaction region. They have also deduced that the effectiveness of the collective interactions of a monoenergetic, low angular divergence IREB increases with the plasma density [50,51].

# VI. NIIEFA EXPERIMENTAL RESEARCH—TWO-STREAM INSTABILITY

NIIEFA's experiments, under the leadership of L. V. Dubovoy, provided important information on "reverse current enhancement" (two-stream instability) in the propagation of an IREB through air. The research was published in 1977 [32,33] with references to earlier research dating back to 1973 [52,53] with no new publications since 1977.

A 1.5 MeV, 50 kA, 16 ns electron beam from the REP-5 accelerator was injected into air and nitrogen at pressures from $10^{-2}$ to 760 Torr. Most of the investigations were carried out well below the pressure of 1 Torr where the two-stream instability comes into play. But measurements were also performed at atmospheric pressure in air. The characteristics of the propagating beam were measured at $z$ = 60 cm and 1.2 m.

The investigation focused on the case in which the amplitude of the current induced in plasma by the IREB pulse was higher than the beam current pulse amplitude. This condition was called reverse current enhancement (or RCE effect). The RCE effect was present only in the case where the electron beam has a large energy spread.

A typical electron beam current pulse scan is shown in Fig. 50 demonstrating the beam current $I_b(t)$, total current $I_T(t)$, and reverse

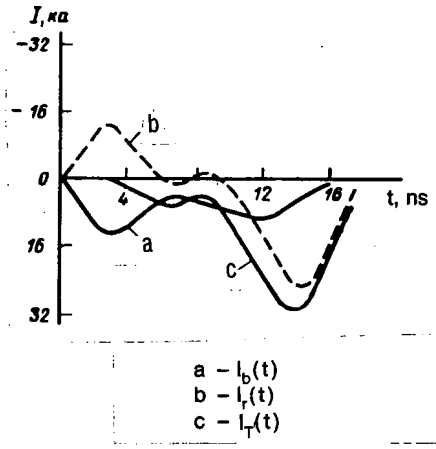


Fig. 50—Beam current pulse scan [33]

current $I_r(t)$, where $I_r(t) = I_T(t) - I_b(t)$ for a pressure of 0.05 Torr [33]. Figure 51 demonstrates the dependence of the basic parameters observed in this reverse current process upon the background gas pressure [33].

From the experimental results, NIIEFA researchers noted that the reverse current $I_r$ can be larger than the beam current $I_b$ with the maximum (as shown for maximum y in Fig. 51) found at a pressure of 0.03 Torr marked by a maximum in the beam energy spread ($\Delta E$) and a maximum loss in the energy of the beam.

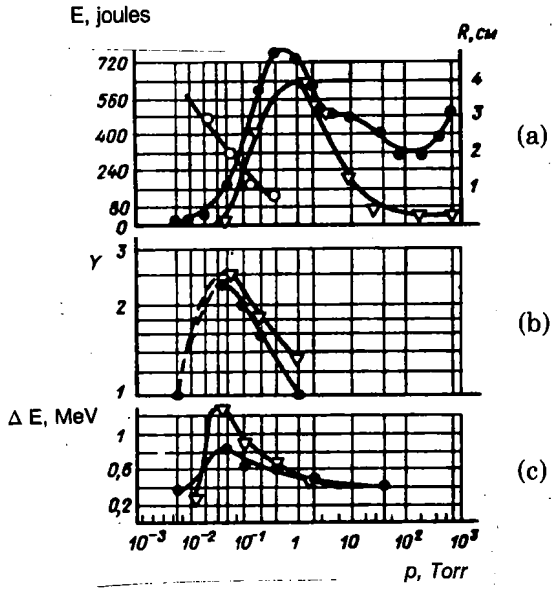


• – z = 60 cm ▽ – z = 1.2 m
a – beam energy E(f)p, here o – beam radius $r_b$(f)p
b – Y(p) = ($I_r/I_b$)(p)
c – ΔE(p) change in energy of the beam spectra

Fig. 51—Dependence of system parameters upon background gas pressure [33]

# VII. NIITP EXPERIMENTAL RESEARCH—IREB INJECTION INTO ATMOSPHERIC AIR

From 1977 to 1981 the NIITP carried on a seemingly minor effort (represented by two published papers and four authors) under the leadership of V. M. Iyevlev. A 500 keV CW electron beam was injected into air at atmospheric pressure through a differential pumping system instead of a titanium foil window [54,55]. Special attention was given to the development of the differential pumping system utilizing a series of apertures with various pumping schemes incorporated between each aperture in order to reduce the gas load and provide a smooth transition between the atmospheric air and the high vacuum required in the accelerator section.

The maximum propagation distance of 200 keV electrons through atmospheric air was only about 30 cm. However, as the air was heated up by the beam, a lower density channel formed, extending the propagation distance. No further information was published on the details of beam propagation through atmospheric air.

Stated practical applications of the research were beam welding, cutting, and hole boring of solid materials.

# VIII. VEI RESEARCH—THEORY AND EXPERIMENT

VEI researchers have recently performed extensive research on IREB transport through low-pressure background gases ($10^{-3}$ to $10^{-5}$ Torr), as described in a previous report [1]. In high gas pressure, IREB propagation studies that began in 1979 are still in progress. VEI researchers, under the leadership of A. V. Zharinov and M. A. Vlasov, concentrated on the study of the propagation windows for IREB transport, the determination of the upper limit of gas pressure to maintain a plasma-beam discharge (plasma formed by IREB injected into air), injection methods of an IREB into the atmosphere using differential pumping, the formation of large microwave signals inherent in the beam, and the formation of positively charged electron beams. The latter of these seems to be of interest because the researchers claim that the beam does not become subjected to any irregular instabilities and is axially self-centering.

The upper limit of the gas pressure for a plasma-beam discharge was experimentally determined in [56] at VEI using a 300 keV, 20 A, 400 $\mu s$, 0.6 cm diameter electron beam and injecting the beam into air through a differential pumping system. The pressure range used was 0.1 to 300 Torr. It was determined that in the pressure range 50 to 300 Torr the electron beam propagation through the dense air was stable and that the dynamics of the beam radius change along the length and time of propagation can be well approximated by the gas collision theory.

Researchers at VEI have investigated the decrease in the number of neutral gas atoms in the path of the plasma channel due to the effect of the hydrodynamic expulsion of the channel hot gas [57,56]. Here the interaction of the IREB with the background gas has been investigated showing the basic mechanism to be the dissipation of energy due to electron collisions with the background gas particles whereby plasma is formed and the gas is heated up.

The gas temperature was estimated from the following expression

$$T \sim (\rho_a I_b)^{0.2}$$

where $\rho_a$ = the initial gas density

$I_b$ = beam current.

For pressures of 10 to 40 Torr, the value of $T$ was found to be 0.4 to 0.5 eV for the observed beam parameters; the concentration of neutrals inside the channel was calculated to be 2.5 to 8 $\times$ $10^{16}$ $cm^{-3}$ [56].

VEI researchers carried out experiments in 1984 [58] on the formation of a beam-plasma discharge in the area where the electron beam was injected into the atmosphere through a differential pumping system. The energy of the beam was 300 keV, beam current 27 A, pulse length 500 $\mu s$, and diameter 0.6 cm. The beam transport was stable through the differentially pumped beam injection area where the plasma density had an extended gradient and the gas pressure changed from 20 to 400 Torr.

The interaction of the electron beam with the background gas in this area led to the heating of the gas and the gas radial expansion, which generated a cylindrical shock wave. The latter was reflected off the walls, collapsed onto the axis, and radially expanded. Because of the gas heating, a gas plug was formed in the channel and obstructed the gas flow. It was demonstrated that because of the conditions set up by the gas density gradient along the beam axis, a plasma-beam discharge was created with microwave radiation in the 3 cm wavelength region.

VEI researchers in 1984 also described a differential pumping system they have designed for the injection of an electron beam from a pressure of $10^{-5}$ Torr to a region under pressure of 10 to 100 Torr [59].

An interesting finding of the recent VEI research was the formation of overall positively charged beams of electrons [60,61]. These beams had an overabundance of positive charge in the neighborhood of $10^3$ to $10^4$ V and could be varied as required by changing either the pressure or the type of background gas or metal vapor. The critical current was shown to increase several hundred fold (over 10 A) using gridded conducting tubes for propagation. The electric fields in this case could be higher than in the quasi-neutral case (when $n_i = n_e$, $\tau_i = \tau_e$) by factors of 100 to 1000. The main advantage of positively charged electron beams is that they are not subject to irregular instabilities and have no beam current limits because of these instabilities and are also axially self-centering, which may allow them to be easily transported along various configurations of metal beam pipes [60]. The formation of this type of electron beam is explained by VEI researchers using the apparatus shown in Fig. 52 [60]. The electron beam flows with a beam current $I_b$, velocity $v = \beta c$ along the axis of a tube of length $L$ and radius $R$ as shown in the figure. A potential $V_T$ is applied to the tube, which is negative with respect to other electrodes that contact the plasma created by the beam. All the secondary electrons created by the beam inside the tube have to leave by the ends, and all the ions

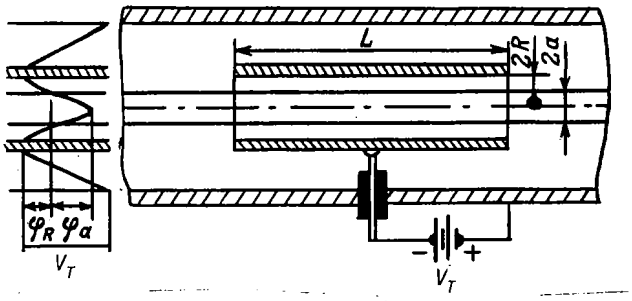


Fig. 52—Apparatus for the formation of positively charged electron beams showing the voltage radial distribution [60]

must flow to the walls under the action of the field $E_r$ where they recombine at the wall surface. For the secondary electrons to leave the tube, the voltage on the tube $V_T$ must be greater than the voltage between the beam boundary and the inside of the tube $\varphi_R$ (as shown in the voltage distribution plot in Fig. 52). The condition for the electron beam to pass through the tube must be met: Here the kinetic energy of the beam $\varphi_o$ must be larger than $V_T - \varphi_R$. The calculations in Ref. 60 demonstrate that this sort of overcompensated electron beam can indeed be formed and could be of future interest because of its aforementioned advantages.

VEI also considered the practical aspects of the electron beam for processing of materials [57,62], involving the injection of 0.5 MeV beam into air at atmospheric pressure. It was found that electron beam propagation is very weakly dependent upon beam current ($L \sim I_b^{1/15}$) but strongly dependent upon beam energy ($L \sim E_b^{2/3}$). Beam energies of the order of 0.5 MeV were recommended for processing of materials. Even at this energy, the propagation distance was about 0.6 cm. The researchers also mention that energy transport by means of an electron beam, while taking into account scattering and gas heating, still has not been investigated sufficiently [57].

# IX. MFTI RESEARCH ON BEAM INSTABILITY

Researchers of the Moscow Physico-Technical Institute (MFTI), under the leadership of K. V. Khodatayev, carried out investigations from 1973 to the present on the theory of the resistive hose instability and the development of beam oscillations and noise.

A nonlinear solution to the sausage mode (azimuthal quantum number m = 0) of the resistive instability was determined in 1984 [63] for an IREB passing through a conducting plasma. It was determined that the sausage mode of the instability actually does develop. In the case of a Bennett distribution function, the sausage mode of the resistive instability has been observed to be dampened.

Using different values of exitation frequencies, these calculations showed that phase mixing leads to complete damping of the sausage mode of the resistive instability in the case of a hot beam with a Bennett density distribution. According to MFTI researchers, this conclusion holds true in conjunction with the experimental results of Refs. 64 and 65 in which the hose instability with mode m = 1 was observed, but where there was no observation of the sausage mode of the resistive instability.

MFTI researchers have looked at the energy of beam noise as a function of time. They have seen this beam noise mount rapidly, reach a saturation, and then slowly decrease with time [66]. They have determined that the beam distribution gradually stops varying, the high frequency oscillations become dampened, and these oscillations transfer their energy to the thermal movement of the beam particles. Here the beam emittance, which is the characteristic of the thermal energy of the beam, begins to increase.

Equations of nonequilibrium states of a hot ribbon electron beam moving through a stationary ion background indicate that the beam relaxes to an equilibrium condition. That process was broken down into two cases. In the first case, the transformation took place in conjunction with the collisionless theory in which the phase mixing of electron trajectories led to a large modulation of the beam distribution function. The calculations showed that this quenches the oscillations of the macroscopic beam characteristics. In the second case, reversible processes smooth out the inhomogeneities of the distribution function in phase space, and thus produce beam relaxation.

The characteristic time for beam relaxation was determined to be the electron oscillation period. The rate of oscillation damping of the

macroscopic beam characteristics depends upon the type of initial excitation of the beam distribution. Small amplitude oscillations, which represent a fairly small area of the phase space, are damped slower than the large excitations, which possess a larger phase space [66].

# X. IEM RESEARCH

Researchers at the Institute of Experimental Meteorology (IEM) in Obninsk were working on the transport of IREBs through neutral gases in 1980–1981 [67,68]. In their theoretical studies, they have analyzed a condition of self-channeling of the electron beam where the action of the beam's self-magnetic field is capable of considerably decreasing the beam's spreading due to multiple scattering. In these investigations, an example was chosen with a 20 MeV, 34 kA electron beam transported in air with a density of $1.3 \times 10^{-4}$ g/cm$^3$ with an initial beam cross section of 100 cm$^2$. It was determined that the cross sectional area at 100 meters increased a factor of 4.5. When the beam current was taken at low values ($I_b$ = 100 A), however, this value increased a factor of 3 for all other conditions unchanged [67].

These researchers reached the following conclusions [67]:

1. The condition of self-channeling is analogous to the equilibrium case for the pinch effect where the transverse energy of the beam particles acts as the temperature.
2. The effect of the beam's self-magnetic field can considerably decrease beam spreading caused by multiple scattering.
3. Even with self-channeling, the beam spreads; initially this follows an exponential law.

These observations, however, have been well documented by Western sources in the early 1960s and 1970s.

# XI. CONCLUSIONS

Soviet research on the propagation of intense relativistic electron beams appears to be broad and systematic, and it has gathered momentum during the past five years. One obvious application of such research is in the area of inertial fusion reactors driven by electron beams. Another is to resolve a problem in the quest for the charged-particle beam weapon—the feasibility of efficiently transporting such beams through atmospheric air. The data presented here and drawn from open Soviet publications are pertinent to some basic issues of beam weapon research. However, they cannot be directly attributed to such research, primarily because of the low beam energies (< 1.5 MeV), short propagation distances (< 3 m), and low pressures used in the published Soviet experiments.

An indirect hint of a possible military involvement is the disappearance from published journals of five key experimental teams during the period 1978 to 1981, including a IYaF-TPI team lead by Yu. P. Usov and two teams at KhFTI led by Ya. B. Faynberg, Yu. V. Tkach, and A. K. Berezin (see Fig. 1). If the disappearance of these teams was due to security classification, then the total Soviet effort in this research area may be much larger than appears in the published literature. Even in the absence of publications from the five experimental research teams, the overall number of Soviet published papers has steeply increased since 1983, and the number of authors has shown a similar increase since 1980 (see Fig. 2).

Five new Soviet research efforts, initiated in the late 1970s or early 1980s, are currently active in IREB propagation studies. Of these, FIAN-IOF, led by A. A. Rukhadze, demonstrates the largest experimental effort; the largest theoretical effort is being carried out at IYaF-TPI under the leadership of V. P. Grigor'yev.

Because the research being carried out by the new research teams was basically the same as that of the five old teams, two hypotheses are offered:

1. The entire research program has been transferred to the new teams, while the old team membership has been disbanded.
2. The new teams assumed only the part of the program suitable for open publication, and the old teams commenced a new, advanced phase of research subject to classification.

The second hypothesis is more probable, because of the total absence of the previous authors in the literature of the 1980s. It is unlikely that disbanded team members would altogether cease contributing to scientific research.

The specific research issues pursued in the published literature by the former and the new Soviet research teams on IREB propagation through air for the past 15 years are as follows:

- The formation of a plasma channel created by an IREB propagating through background air and the investigation of the effect of beam parameters upon the plasma channel parameters (and vice versa).
- Determination of the background air pressure for the optimum transport of an IREB. Two optimum pressure ranges were determined:
  - The "ion focused regime"—0.06 to 0.09 Torr.
  - The "low pressure window"—1 Torr.
- The current enhancement effect, whereby the current induced in the plasma by the IREB is larger than the original beam current.
- The effect of the resistive hose instability upon IREB propagation.

These key issues of Soviet research match the main interests of U.S. research on IREB propagation through high pressure air.

Soviet researchers found that an IREB can be transported in large volume, large diameter insulating channels, and through free space by forming two channels for the return current flow: one in the beam and the other in a thin cylindrical layer around the beam. The latter shorts the beam current to the accelerator while maintaining beam self-focusing; and the plasma layer has a stabilizing effect upon the lateral oscillations of the beam, thus improving IREB transport. This layer was assumed to be a plasma channel carrying part of the return current of the beam. When the beam developed hose instability, the cylindrical symmetry of the layer was not disturbed, but the entire beam was observed to be displaced laterally. Measurements revealed that no high energy electrons moving parallel to the beam flow were present in this layer region. It was determined that the plasma channel was produced by the ionization of the background gas by electrons of the IREB leading front, and the beam trajectory was determined by the movement of the low energy electrons and not by the main part of the beam. The plasma channel remained intact longer than 100 ns. The beam was also found capable of tracking the plasma channel.

In their investigation of "current enhancement," Soviet researchers discovered that most of the plasma current density $J_p$ flowed within

the confines of the electron beam in a time about 100 ns, which is considerably longer than the beam pulse. The return current enhancement (RCE) effect was found to be present only in the case where the IREB had a large energy spread. The limitations of the "two-stream instability" at the low pressure of IREB propagation has been reported only by NIIEFA, and the earlier Soviet reports have mentioned that all current enhancement is due to the two-stream instability. However, in 1984, FIAN-IOF researchers observed a current enhancement condition that takes place at pressures close to atmospheric when none of the earlier studied causes of current enhancement could be the reason for the effect. This anomalous current enhancement was found to increase with pressure and propagation length and was in the direction of the IREB. The Soviet researchers claim that they are currently making further studies of this effect.

In the Soviet open literature, the only mention of laser guidance (the use of a laser to create a low-pressure channel along whose axis an IREB can propagate) was made in 1974 at FIAN-IOF by G. A. Askar'yan [69]. Here a preliminary experiment demonstrated the formation by a laser of a low-density channel in air. This channel had a finite lifetime of several hundreds of microseconds with a density 10 to 20 times lower inside the channel. A 50 keV electron beam pulse was passed through this channel successfully, thus demonstrating laser guidance. Other FIAN-IOF papers published by G. A. Askar'yan and his co-workers have made statements on the use of laser guidance for the successful transport of charged particle beams. There are no recent publications on laser guidance, and it is believed that this subject is censored by the Soviet authorities.

Most of the Soviet reports that have been considered here do not specifically mention a single application of their research. However, many papers generally indicate the importance of optimum propagation conditions for high energy, high current beams, and their transport to a maximum allowable distance. In a few cases (VEI, NIITP, MFTI), where the injection of the beam into atmospheric pressure air was considered, specific applications for beam welding, beam cutting, and specimen hole boring were mentioned along with the general objective of achieving maximum propagation length in air.

# Appendix

## SOVIET RESEARCH TEAMS INVOLVED IN IREB PROPAGATION

Soviet research teams involved in IREB propagation in air at pressures from 0.1 to 760 Torr are listed below by institute affiliation. Group leaders are indicated in italics.

IYaF-TPI: Institute of Nuclear Physics at Tomsk Polytechnic Institute, Tomsk

Team 1: Theory and Computer Simulation

*V. P. Grigor'yev*
A. G. Potashev, N. S. Shulayev, A. V. Zakharov
A. I. Koryakin, A. S. Popov, A. N. Didenko
G. P. Isayev

Team 2: Experimental

*Yu. P. Usov*
A. N. Didenko, V. A. Tuzov, A. I. Ryabchikov
Ya. Ye. Krasik, A. V. Petrov, G. I. Kotlyarevskiy

IAE: Kurchatov Institute of Atomic Energy, Moscow

*L. I. Rudakov*
V. P. Smirnov, V. V. Gorev, S. V. Zakharov
L. Ye. Aranchuk, V. D. Vikharev, S. F. Zhandarov
V. D. Korolev, L. I. Urutskoyev, S. F. Grigor'yev
A. V. Gordeyev, V. V. Zazhivikhin, V. Yu. Shuvayev

FIAN: Lebedev Physics Institute/IOF: Institute of General Physics, Moscow

*A. A. Rukhadze*
A. A. Savin, G. P. Mkheidze, A. L. Ipatov
G. A. Askar'yan, B. M. Manzon, R. R. Kikvidze
I. M. Minayev, A. G. Shkvarunets, V. Yu. Shafer
S. N. Kabanov, A. A. Korolev, A. I. Kuz'min
V. Ye. Kul'beda, V. Yu. Nosach

KhFTI: Physical-Technical Institute, Khar'kov

Team 1

*Ya. B. Faynberg*
*Yu. V. Tkach*
I. I. Magda, G. V. Skachek, S. S. Pushkarev

| | | |
|---|---|---|
| V. A. Bondarenko | I. P. Panchenko | B. D. Panasenko |
| S. I. Naysteter | I. N. Onishchenko | V. I. Shevchenko |
| P. M. Lebedev | | |

Team 2

*Ya. B. Faynberg*
*A. K. Berezin*

| | | |
|---|---|---|
| V. A. Kiselev | V. P. Zeydlits | I. A. Grishayev |
| B. G. Safronov | G. L. Fursov | I. N. Onishchenko |
| N. M. Zemlyanskiy | I. K. Nikol'skiy | V. I. Mirnyy |
| L. I. Bolotin | S. S. Krivulya | A. M. Yegorov |
| V. A. Buts | V. I. Kurilko | A. P. Tolstoluzhskiy |

NIIEFA: Yefremov Institute of Electrophysical Equipment, Leningrad

*L. V. Dubovoy*

| | | |
|---|---|---|
| T. S. Gosteva | G. R. Zablotskaya | B. A. Ivanov |
| V. I. Chernobrovin | S. A. Kolyubakin | |

NIITP: Scientific Research Center of Thermal Processes, Moscow

*V. M. Iyevlev*

| | | |
|---|---|---|
| A. S. Koroteyev | V. V. Koba | I. G. Kulakov |

VEI: All-Union Electric Engineering Institute, Moscow

*A. V. Zharinov*
*M. A. Vlasov*

| | | |
|---|---|---|
| S. V. Nikonov | S. I. Vybornov | V. A. Safonov |
| A. V. Rykhlov | V. P. Popovich | Yu. A. Yel'chin |
| V. A. Artemov | L. G. Dubas | I. P. Denisova |
| A. V. Smirnov | | |

MFTI: Moscow Physico-Technical Institute, Moscow

*K. V. Khodatayev*

| | | |
|---|---|---|
| V. G. Leyman | A. A. Ivanov | K. G. Gureyev |
| V. O. Zolotarev | S. D. Stolbetsov | N. Ye. Rozanov |
| N. S. Putvinskaya | O. B. Ovsyanikova | F. F. Kamenets |

IEM: Institute of Experimental Meteorology, Obninsk

*A. P. Budnik*
P. N. Svirkunov

# REFERENCES

The following abbreviations are used in the references.

| | |
|---|---|
| AE | *Atomnaya energiya* |
| FP | *Fizika plazmy* |
| Fiz i khim OM | *Fizika i khimiya obrabotki materialov* |
| IVUZ: fiz | *Izvestiya vysshikh uchebnykh zavedeniy MV i SSO SSSR: fizika* |
| Izv AN SSSR, ser. EiT | *Izvestiya Akademii nauk SSSR, Seriya energetika i transport* |
| Izv AN SSSR, ser. fiz. | *Izvestiya Akademii nauk SSSR, Seriya fizicheskaya* |
| Izv AN SSSR, ser. tekh. nauk | *Izvestiya Akademii nauk SSSR, Sibirskoe otedelenie, Seriya tekhnicheskikh nauk* |
| KE | *Kvantovaya elektronika* |
| PTE | *Pribory i tekhnika eksperimenta* |
| UFZh | *Ukrainskiy fizicheskiy zhurnal* |
| ZhETF | *Zhurnal eksperimental'noy i teoreticheskoy fiziki* |
| *ZhETF, Pis'ma* | *Pis'ma v Zhurnal eksperimental'noy i teoreticheskoy fiziki* |
| ZhTF | *Zhurnal tekhnicheskoy fiziki* |
| ZhTF, Pis'ma | *Pis'ma v Zhurnal tekhnicheskoy fiziki* |


1. Wells, Nikita, *Transport of Intense Relativistic Electron Beams Through Low Pressure Air in the USSR*, The RAND Corporation, R-3309-ARPA, August 1986.
2. Kassel, Simon, and Charles D. Hendricks, *High-Current Particle Beams I. The Western USSR Research Groups*, The RAND Corporation, R-1552-ARPA, April 1975.
3. Kotlyarevskiy, G. I., A. I. Ryabchikov, Yu. P. Usov, "An Experimental Observation of the Disruption of a High-Current Beam During Transport in a Dense Gas," FP, Vol. 2, No. 4, 1976, p. 689.
4. Grigor'yev, V. P., A. S. Popov, A. G. Potashev, N. S. Shulayev, "Features of Plasma Channel Formation in Long Drift Tubes," ZhTF, Vol. 50, No. 6, 1980, p. 1208.

5. Grigor'yev, V. P., A. G. Potashev, N. S. Shulayev, "Numerical Simulation of Plasma Channel Formation with Injection of an Intense Electron Beam into a Neutral Gas," FP, Vol. 5, No. 2, 1979, p. 376.
6. Grigor'yev, V. P., A. I. Koryakin, A. G. Potashev, "A Numerical Simulation of the Formation of a Plasma Channel and the Dynamics of a High-Current Electron Beam with Injection into a Neutral Gas," FP, Vol. 10, No. 4, 1984, p. 783.
7. Rudakov, L. I., V. P. Smirnov, A. M. Spektor, "The Behavior of a High-Current Electron Beam in Dense Gas," ZhETF, Pis'ma, Vol. 15, No. 9, 1972, p. 540.
8. Mehr, F. J., M. A. Biondi, "Electron Temperature Dependence of Recombination of $O_2^+$ and $N_2^+$ Ions with Electrons," Physical Review, Vol. 181, 1969, p. 264.
9. Ginzburg, V. L., "Rasprostraneniye elektromagnitnykh voln v plasme," M., "Nauka," 1969, Chapter 2, Section 6.
10. Grigor'yev, V. P., A. N. Didenko, N. S. Shulayev, "Stationary State of an Electron Beam in a Plasma Channel with Return Current," ZhTF, Vol. 48, No. 7, 1978, p. 1326.
11. Rukhadze, A. A., V. G. Rukhlin, "Injection of a Relativistic Electron Beam into a Plasma," ZhETF, Vol. 61, No. 1, 1971, p. 177.
12. Kingsep, S. S., I. V. Novobrantsev, L. I, Rudakov, V. P. Smirnov, A. M. Spektor, "The Mechanism Involved in the Ionization of Gas by an Intense Electron Beam," ZhETF, Vol. 63, No. 6, 1972, p. 2132.
13. Petrov, A. V., A. I. Ryabchikov, V. A. Tuzov, Yu. P. Usov, "Features of the Transport of a High-Current Relativistic Electron Beam," IVUZ—fiz, No. 7, 1978, p. 144.
14. Didenko, A. N., Ya. Ye. Krasik, A. V. Petrov, A. I. Ryabchikov, V. A. Tuzov, Yu. P. Usov, "An Investigation of the Dispersion of a High-Current Relativistic Electron Beam in a Transverse Magnetic Field," FP, Vol. 3, No. 5, 1977, p. 1128.
15. Kotlyarevskiy, G. I., Yu. P. Usov, "The Energy Spectrum of a High-Current Electron Beam Transported in a Neutral Gas," ZhTF, Vol. 48, No. 3, 1978, p. 490.
16. Kotlyarevskiy, G. I., Yu. P. Usov, "The Energy Spectrum Time Structure of a High-Current Relativistic Electron Beam," ZhTF, Vol. 46, No. 7, 1976, p. 1550.
17. Kotlyarevskiy, G. I., Yu. P. Usov, "Regulating the Current Pulse Length of a High-Current Relativistic Electron Beam," ZhTF, Vol. 47, No. 9, 1977, p. 1981.
18. Baranchikov, Ye. I., A. V. Gordeyev, V. D. Korolev, L. I. Rudakov, V. P. Smirnov, "Distribution of an Intense Electron Beam Along Plasma Channels," FP, Vol. 4, No. 4, 1978, p. 773.

19. Rudakov, L. I., "Transport of an REB to a Thermonuclear Target," FP, Vol. 4, No. 1, 1978, p. 72.
20. Aranchuk, L. Ye., V. D. Vikharev, V. V. Gorev, S. F. Zhandarov, S. V. Zakharov, V. D. Korolev, V. P. Smirnov, L. I. Urutskoyev, "Resonant Resistive Instability of a High-Current Relativistic Electron Beam in a Plasma," ZhETF, Vol. 86, No. 4, 1984, p. 1280.
21. Aranchuk, L. Ye, V. D. Vikharev, V. V. Gorev, S. F. Zhandarov, S. F. Zakharov, V. D. Korolev, L. I. Rudakov, V. P. Smirnov, L. I. Urutskoyev, "Resonant Resistive Instability of a Relativistic Electron Beam in Plasma," ZhETF, Pis'ma, Vol. 36, No. 9, 1982, p. 331.
22. Gorev, V. V., S. F. Grigor'yev, S. V. Zakharov, "Resonant Resistive Instability of a Charged Particle Beam in Plasma with a Longitudinal Magnetic Field," FP, Vol. 10, No. 6, 1984, p. 1253.
23. Gorev, V. V., S. V. Zakharov, "The Self-Focusing of a Charged Particle Beam in an Inhomogeneous Plasma," FP, Vol. 11, No. 1, 1985, p. 96.
24. Gordeyev, A. V., V. V. Zazhivikhin, "Resonant Helical Instability of a High-Current Electron Beam," FP, Vol. 10, No. 2, 1984, p. 272.
25. Gordeyev, A. V., L. I. Rudakov, "The Electromagnetic Instability of a Charged-Particle Beam in a Dense Plasma," ZhETF, Vol. 83, No. 6, 1982, p. 2048.
26. Gordeyev, A. V., L. I. Rudakov, V. Yu. Shuvayev, "The Displacement of a Magnetic Field by a Hot Electron Cloud," ZhETF, Vol. 85, No. 1, 1983, p. 155.
27. Ipatov, A. L., S. N. Kabanov, A. A. Korolev, A. I. Kuz'min, V. Ye. Kul'beda, G. P. Mkheidze, V. Yu. Nosach, A. A. Rukhadze, A. A. Savin, "An Investigation of the Change in Neutral Gas Density During the Transport of a Relativistic Electron Beam Pulse," ZhTF, Pis'ma, Vol. 10, No. 3, 1984, p. 162.
28. Gailov, V. A., V. Ya. Karpov, A. Yu. Krukovskiy, "The Calculation of the Development of An Axisymmetric Hot Explosion in a Molecular Gas," Preprint IVTAN No. 5-138, M., 1984.
29. Askar'yan, G. A., G. P. Mkheidze, A. A. Savin, "The Determination of Energy Deposition from High-Current Beams by Pulse Excitation and Density Decrease of the Gas During REB Transport," ZhTF, Pis'ma, Vol. 10, No. 23, 1984, p. 1465.
30. Arutyunyan, S. G., O. V. Bogdankevich, Yu. F. Bondar', A. A. Rukhadze, S. I. Zavorotnyy, A. L. Ipatov, G. P. Mkheidze, A. A. Ovchinnikov, "The Transport of an Intense Electron Beam in a Neutral Gas," KE, Vol. 9, No. 2, 1982, p. 234.

31. Bondar', Yu. F., S. I. Zavorotnyy, A. L. Ipatov, G. P. Mkheidze, A. A. Ovchinnikov, A. A. Savin, "A Study of a Relativistic Electron Beam in a Dense Gas," FP, Vol. 8, No. 6, 1982, p. 1192.
32. Gosteva, T. S., L. V. Dubovoy, G. R. Zablotskaya, B. A. Ivanov, V. I. Chernobrovin, "The Transport of Precritical Current Relativistic Electron Beams in Rarefied Gas and Plasma," FP, Vol. 4, No. 2, 1978, p. 460.
33. Gosteva, T. S., L. V. Dubovoy, G. R. Zablotskaya, B. A. Ivanov, V. I. Chernobrovin, "An Increase in the Reverse Current in the Interaction of an Intense Relativistic Electron Beam with a Gas Target," FP, Vol. 3, No. 6, 1977, p. 1261.
34. Briggs, R. J., J. C. Clark, et al., Proc. 2nd Int. Conf. High-Power Electron Beam Research and Technology, Vol. 1, 1977, Ithaca, N.Y., p. 319.
35. Wachtel, J. M., S. Safran, "Current Amplification in a Relativistic Electron Beam," Physical Review Letters, Vol. 32, No. 3, 1974, p. 95.
36. Ipatov, A. L., G. P. Mkheidze, A. A. Savin, "Current Increase During the Interaction of a Relativistic Electron Beam with a Neutral Gas," ZhTF, Pis'ma, Vol. 10, No. 11, 1984, p. 681.
37. Zavorotnyy, S. I., O. V. Karpov, V. Ye. Muzalevskiy, A. A. Ovchinnikov, A. A. Savin, "Experimental Investigation of Beam Plasma Concentration and Temperature by a Method of Laser Scattering," ZhTF, Vol. 53, No. 8, 1983, p. 1466.
38. Mkheidze, G. P., A. A. Savin, G. A. Sorokin, "Pulse Front Erosion of an REB in a Neutral Gas," ZhTF, Vol. 55, No. 7, 1985, p. 1465.
39. Kikvidze, R. R., I. M. Minayev, A. A. Rukhadze, A. G. Shkvarunets, "Transport of an REB Through High Pressure Gas at Intermediate Current Densities," FP, Vol. 10, No. 5, 1984, p. 976.
40. Tkach, Yu. V., I. I. Magda, G. V. Skachek, S. S. Pushkarev, I. P. Panchenko, "The Transport of an Intense Relativistic Electron Beam Through Gas," ZhTF, Vol. 44, No. 3, 1974, p. 658.
41. Tkach, Yu. V., I. I. Magda, G. V. Skachek, S. S. Pushkarev, V. A. Bondarenko, V. D. Panasenko, S. I. Naysteter, "The Relaxation of an Intense Relativistic Beam in Plasma," FP, Vol. 6, No. 3, 1980, p. 586.
42. Bondarenko, V. A., I. I. Magda, B. D. Panasenko, S. S. Pushkarev, G. V. Skachek, "Nonstationary Nature of the Angular Spectrum and Radial Density Distribution of a Relativistic Beam in Neutral Gas," FP, Vol. 8, No. 4, 1982, p. 797.
43. Berezin, A. K., Ya. B. Faynberg, L. I. Bolotin, A. M. Yegorov, V. A. Kiselev, V. A. Buts, V. I. Kurilko, A. P. Totstoluzhskiy, "The

Interaction of a Modulated Relativistic Electron Beam with Plasma," ZhETF, Vol. 63, No. 3, 1972, p. 861.

44. Berezin, A. K., Ya. B. Faynberg, L. I. Bolotin, A. M. Yegorov, V. A. Kiselev, "Experimental Investigation of the Interactions of Modulated Relativistic Electron Beams with Plasma," ZhETF, Pis'ma, Vol. 13, No. 9, 1971, p. 498.
45. Berezina, G. F., Ya. B. Faynberg, A. K. Berezin, V. P. Zeydlits, "On the Interaction of a Plasma and an Electron Beam Modulated by Low-Frequency Oscillations," ZhETF, Vol. 62, No. 6, 1972, p. 2115.
46. Kiselev, V. A., Ya. B. Faynberg, A. K. Berezin, "The Collective Interaction of a Relativistic Electron Beam with a Dense Plasma," ZhETF, Pis'ma, Vol. 20, No. 9, 1974, p. 603.
47. Kiselev, V. A., A. K. Berezin, Ya. B. Faynberg, I. K. Nikol'skiy, "The Interaction of a Relativistic Electron Beam with a Dense Plasma," ZhTF, Pis'ma, Vol. 2, No. 2, 1976, p. 53.
48. Kiselev, V. A., A. K. Berezin, Ya. B. Faynberg, "The Interaction of a Relativistic Electron Beam with a Dense Plasma," ZhETF, Vol. 71, No. 1, 1976, p. 193.
49. Kiselev, V. A., A. K. Berezin, Ya. B. Faynberg, V. P. Zeydlits, "The Interaction of a Monoenergetic Relativistic Electron Beam with a Plasma Formed in the Atmosphere," ZhETF, Pis'ma, Vol. 29, No. 12, 179, p. 762.
50. Berezin, A. K., I. A. Grishayev, V. P. Zeydlits, V. A. Kiselev, B. G. Safronov, Ya. B. Faynberg, L. G. Fursov, "The Interaction of a Monoenergetic Relativistic Electron Beam, Having Large Gamma, with a Dense Plasma, ZhTF, Pis'ma, Vol. 4, No. 12, 1978, p. 732.
51. Berezin, A. K., V. A. Kiselev, Ya. B. Faynberg, "The Interaction of a Monoenergetic Relativistic Electron Beam with a Dense Plasma," UFZh, Vol. 24, No. 1, 1979, p. 94.
52. Gosteva, T. S., G. R. Zablostskaya, B. A. Ivanov, S. A. Kolyubakin, V. I. Chernobrovin, "Spectrograph with Semi-Circular Focusing for the Investigation of the Energy Distribution of an Intense Relativistic Electron Beam," PTE, No. 3, 1975, p. 44.
53. Zablotskaya, G. R., B. A. Ivanov, S. A. Kolyubakin, A. S. Perlin, V. A. Rodichkin, V. B. Shapiro, "An Intense Pulsed Relativistic Electron Beam Accelerator (REP-5) with a 50 kA Beam Current," AE, Vol. 34, No. 6, 1973, p. 471.
54. Iyevlev, V. M., A. S. Koroteyev, "Investigation of High-Current Stationary Electron Beams and Their Injection into the Atmosphere," Izv AN SSR, ser. EiT, No. 3, 1981, p. 3.
55. Iyevlev, V. M., A. S. Koroteyev, V. V. Koba, I. G. Kuklakov, "An Experimental Apparatus for Obtaining a Concentrated Relativistic

Electron Beam in the Atmosphere," Izv An SSSR, ser. tekh. nauk, No. 13, Vyp. 3, 1977, p. 52.
56. Vlasov, M. A., Yu. A. Yel'chin, V. P. Popovich, A. V. Rykhlov, V. A. Safonov, "The Beam-Plasma Discharge with Injection of an Electron Beam into a Dense Gas," ZhTF, Pis'ma, Vol. 10, No. 11, 1984, p. 652.
57. Artemov, V. A., M. A. Vlasov, V. A. Safonov, "The Propagation of an Electron Beam in Gas," Fiz i khim OM, No. 5, 1982, p. 134.
58. Vlasov, M. A., V. P. Popovich, A. V. Rykhlov, V. A. Safonov, A. V. Smirnov, "The Interaction of an Electron Beam with Gas in the Extended Channel of a Differential Pumping System," ZhTF, Vol. 54, No. 8, 1984, p. 1638.
59. Antipov, G. N., F. A. Bagautdinov, S. V. Rybalov, "A Pulsed Differential Pumping System," PTE, No. 6, 1984, p. 150.
60. Zharinov, A. V., M. A. Vlasov, S. I. Vybornov, "Positively Charged Electron Beams," ZhTF, Pis'ma, Vol. 10, No. 19, 1984, p. 1185.
61. Zharinov, A. V., M. A. Vlasov, S. I. Vybornov, "The Stability of Positively Charged Electron Beams," ZhTF, Pis'ma, Vol. 10, No. 19, 1984, p. 1188.
62. Vlasov, M. A., L. G. Dubas, A. V. Zharinov, "The Scattering of an Electron Beam by the Vapor of a Target," Fiz i khim OM, No. 2., 1977, p. 21.
63. Gureyev, K. G., V. O. Zolotarev, S. D. Stolbetsov, "A Kinetic Investigation of the Overstretched Mode of the Resistive Instability of a Relativistic Electron Beam," FP, Vol. 10, No. 6, 1984, p. 1167.
64. Lauer, E. J., R. J. Briggs, T. J. Fessenden, R. E. Hester, E. P. Lee, "Measurements of Hose Instability of a Relativistic Electron Beam," Physics of Fluids, Vol. 21, 1978, p. 1344.
65. Moses, K. G., R. W. Bauer, S. D. Winter, "Behavior of Relativistic Beams Undergoing Hose Motion in a Plasma Channel," Physics of Fluids, Vol. 16, 1973, p. 436.
66. Gureyev, K. G., N. Ye. Rozanov, "The Relaxation of the Non-equilibrium States of an Electron Beam," FP, Vol. 10, No. 6, 1984, p. 1157.
67. Budnik, A. P., P. N. Svirkunov, "The Effect of the Self Magnetic Field of a Charged-Particle Beam on its Propagation in a Neutral Gas," ZhTF, Vol. 51, No. 12, 1981, p. 2506.
68. Buknik, A. P., P. N. Svirkunov, "The Propagation of a Charged-Particle Beam in an Inhomogeneous Medium with the Presence of Radial Forces," ZhTF, Vol. 50, No. 2, 1980, p. 412.

69. Askar'yan, G. A., N. M. Tarasova, "The Passage of Accelerated Particles and Quanta Through Media Along a Lower Density Channel Created by a Laser Beam," ZhETF, Pis'ma, Vol. 20, No. 4, 1974, p. 277.

RAND/R-3463-DARPA